THE UNIVERSITY OF NEW SOUTH WALES
GROUNDWATER CENTRE

and

DEPARTMENT OF LAND & WATER CONSERVATION
CENTRE FOR NATURAL RESOURCES

Investigation of EM31 Anomalies at Yarramanbah / Pump Station Creek, on the Liverpool Plains of New South Wales

WRL RESEARCH REPORT No. 195

Prepared by

R.I. Acworth and R.D. Beasley

April, 1998

Acknowledgments

EXECUTIVE SUMMARY

Detailed investigations have been carried out in the Yarramanbah / Pump Station Creek area, south of Pine Ridge on the Liverpool Plains of New South Wales, to investigate the causes of bulk electrical conductivity anomalies measured with a GEONICS EM-31 in 1994. The EM-31 has been extensively used to map areas at risk of developing dryland salinity as a result of the perceived relationship between shallow saline water tables and salinity hazard.

An area at the north end of the catchment was resurveyed in detail some three and a half years after the initial survey. There was no change in the pattern of the EM-31 data over that period of time.

Areas of high, intermediate, and low bulk electrical conductivity were identified from the EM-31 data and selected for four new test bore sites in 1997. Continuous core was recovered from these test bore sites to depths of approximately 10 m. The cores were cut into 100 mm lengths and a range of physical and chemical tests performed. The source of the bulk electrical conductivity signal measured by the EM-31 was further investigated using a downhole probe (GEONICS EM-39) and by surface conductivity imaging.

The material recovered from the cores was a remarkably uniform smectite clay (montmorillonite) with a little fine sand and coarse sand present. The clays have cation exchange capacities between 80 mE/100g and 110 mE/100g. The moisture contents, measured on a percent dry weight basis, varied between 40% and 110%.

A high correlation (R=0.96) is shown between measurements of bulk electrical conductivity carried out in the borehole using an EM-39, and the fluid conductivity of 1:5 extracts determined on the individual core sub-samples. This correlation is also shown, on a reduced number of samples, by testing the bulk electrical conductivity of the individual cores in the laboratory. Low correlations were shown between bulk electrical conductivity and cation exchange capacity, field moisture content, and clay content, despite significant variations in these parameters.

Field measurements of bulk electrical conductivity, using the surface based electrical conductivity image method, have shown that the bulk electrical conductivity anomaly extends to a depth of between 10 m and 15 m at one of the test bore sites. The edge of the anomaly is relatively sharply defined and has not moved in the three and a half years between the EM-31 surveys.

Chemical analysis of the 1:5 extracts has shown that sodium is the main cation in solution; matched by the chloride, bicarbonate, and sulphate ions. The bulk electrical conductivity anomaly is therefore related to the concentration of salts contained in the interstitial pore space between the clay plates. The lateral variation in bulk electrical conductivity is therefore an indication of the salt distribution in the clay.

The moisture in the clay, particularly the clay containing a high concentration of salts, is effectively held in the clay matrix by surface tension. Clay samples with a porosity of between 50% and 60% remained damp to touch with no free drainage of the moisture. Hydraulic conductivity tests on selected cores indicate values of between 0.08 m/day and 3.3 m/day. This implies that salt can be slowly leached from the clays if a hydraulic gradient is applied. Lateral hydraulic gradients are very low in this part of the Plains.

Hydrochemical analysis of water samples, taken from piezometers completed in the test bores, indicates little if any lateral movement of water. The ratio of sodium to chloride changes from 0.8 for the test bores completed in the high bulk electrical conductivity area, to greater than 2.5 for the bores completed in the low bulk electrical conductivity area. This change in ratio is most likely the result of cation exchange reactions between the interstitial fluid and the clay matrix. Simple evaporative concentration would not change this ratio. It is concluded therefore that evaporation is not a significant process in the formation of these high bulk electrical conductivity zones.

Contents

List of Figures

List of Tables

Chapter 1

INTRODUCTION

1.1 The Dryland Salinity Problem

Salinity has been recognised by the North West Catchment Management Committee and the Liverpool Plains Land Management Committee as the number one land degradation issue faced by managers in the Liverpool Plains of New South Wales. These community organisations have backed funding applications for research projects which, upon completion, should enable a better understanding of salinity processes occurring on the Liverpool Plains. The ultimate aim of the research effort is to develop more appropriate land management practices which will enable the long term sustainability of the abundant natural resources of the region.

The present expression of dryland salinity on the Liverpool Plains is somewhat different from some other parts of New South Wales. Figure 1.1 shows a crop of maize where saline conditions at shallow depth in the soil have severely limited plant growth (Photograph supplied by R. Young, NSW Agriculture). Figure 1.2 shows part of the Dick's Creek catchment between Yass and Canberra, which exhibits more clearly recognised signs of dryland salinity development. The difference in surface expression of dryland salinity has been a complicating factor in the determination of processes and appropriate land management practices.

Electromagnetic induction has been recognised as the *best bet* option for rapid salinity assessment and several statewide projects have been established based upon this technology. Electromagnetic (EM) induction techniques measure the bulk electrical conductivity (σ_a) of the ground. EM techniques are used to map lateral changes in soil bulk conductivity and to help identify soil conditions which lead to the failure of crops as shown in Figure 1.1. Following field testing and coring, EM data sets are interpreted to assess the lateral extent of saline and potentially saline sites. The number and complexity of factors affecting soil (σ_a) have been recently reviewed by Acworth & Jankowski [1], working at Breeza on the Liverpool Plains.

1.1.1 Project Objectives

The main objective of this project was to establish in detail the characteristics of the ground (to a depth of approximately 10 m) associated with σ_a anomalies defined by the GEONICS EM-31 electromagnetic induction meter at a site in the Yarramanbah / Pump Station Creek Catchment.

To meet this objective, extensive data sets of surface EM measurements and surface conductivity image lines have been assembled and compared with conductivity measurements made in four boreholes from

Figure 1.1: Failure of Maize crop on Liverpool Plains due to excess salt in the root zone

Figure 1.2: Dryland salinity in the Dick's Creek catchment between Yass and Canberra

which minimally disturbed core was extracted. The cores were subject to a range of physical and chemical testing.

1.1.2   Project Organisation

This was a collaborative project between the Department of Land and Water Conservation, The University of New South Wales (Water Research Laboratory and the UNSW Groundwater Centre) and community groups in the Liverpool Plains.

Funding was provided jointly by the Department of Land and Water Conservation Centre for Natural Resources, and the UNSW Groundwater Centre.

1.2   Site Location

The study area is part of the Yarramanbah Creek Catchment located in the Upper Eastern Mooki Catchment of the Liverpool Plains, near Quirindi in North Western New South Wales. The site is bounded by latitudes 31°30′ and 31°51′ and longitudes 150°00′ and 150°30′. A location diagram is provided in Figure 1.3.

The Yarramanbah Creek catchment is bounded by the foot slopes of the Liverpool Ranges to the south; Mount Parry and Windy Ridge to the west; and MacDonalds Ridge, Parsons Hill and Middle Range to the east. The lower catchment boundary is taken as the junction of Yarramanbah Creek with Warrah Creek.

1.3   Geology

The Yarramanbah Creek Catchment is part of the regional Gunnedah Basin. The basin has a complex geological history which has been described in detail by Tadros [?]. The Mooki thrust belt forms the eastern margin to the Mooki Valley. Tertiary volcanic activity resulted in the formation of the Liverpool Ranges at the southern edge of the area. The western margin is formed from ridges of older sediments such as the Triassic age Narrabeen Group.

Erosion formed a deeply cut northward flowing drainage system during the Tertiary. This valley system has been extensively filled with a succession of unconsolidated alluvial clays interrupted by alluvial fans forming at the mouth of river systems draining the hills of the Mooki Thrust zone to the east. The unconsolidated material has been sub-divided into a lower, clastic dominant, Gunnedah Formation and an upper, clay dominant, Narrabri Formation (Broughton [3], and Broughton [4]). A detailed interpretation of these deposits is currently being undertaken by Lavitt (pers comm.), who reports that the alluvial fill is best characterised as one of varying sedimentological facies, with some bores showing clay to basement while others show a more complete succession of clastic material with little clay.

This report is concerned with variation in the physical and chemical properties of the top 10 m of alluvial fill, which is predominantly clayey at the site location.
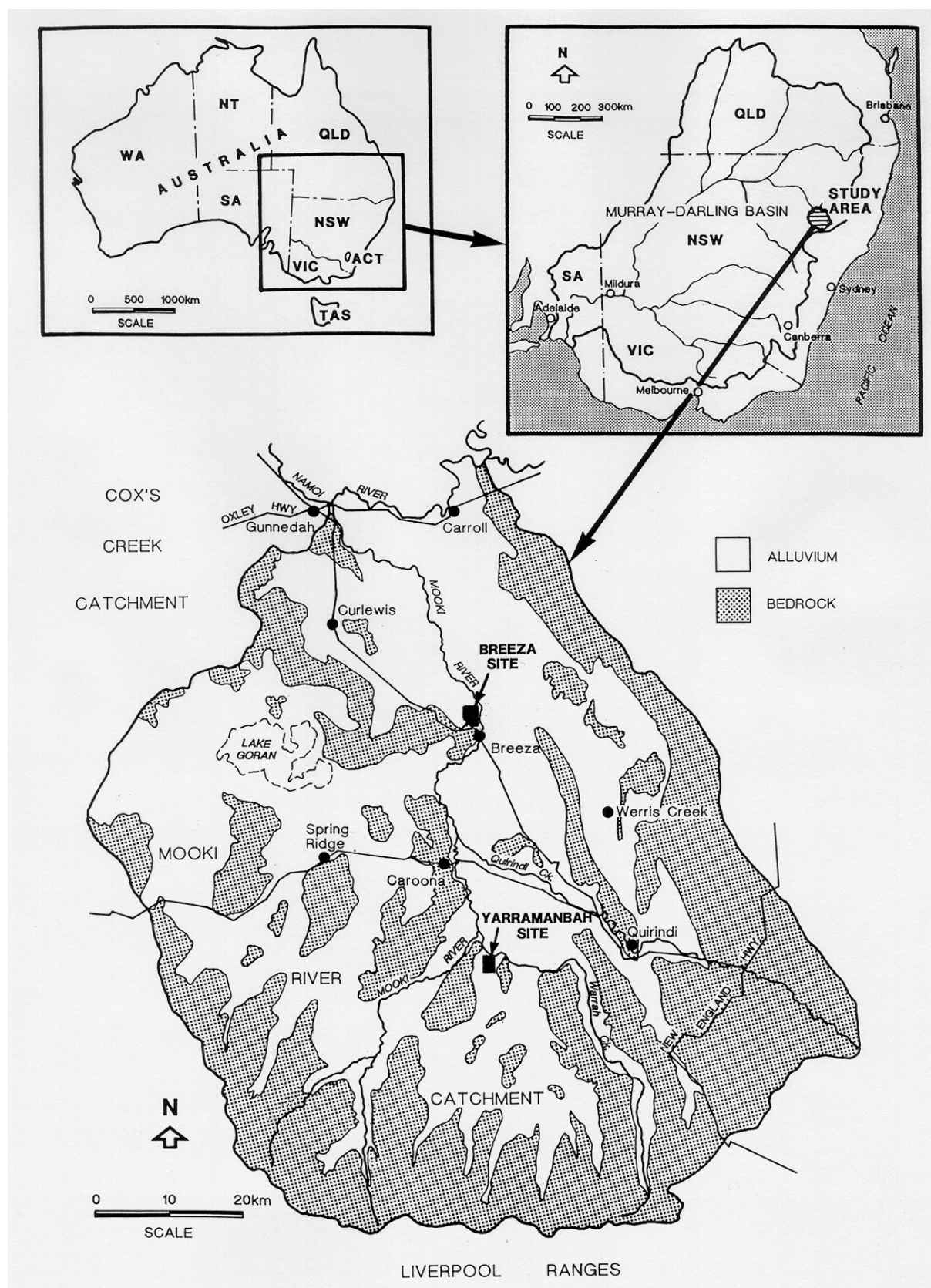
Figure 1.3: Location Map of the Southern Part of the Liverpool Plains

1.4   Soils

Soil landscape units covering Yarramanbah Creek and Pump Station Creek are described in detail by Banks [2] for the Blackville 1:100,000 sheet. Soils are described as very poorly drained self-mulching Grey Vertisols (Grey Clays) in areas of episodic water logging, and very poorly drained self-mulching Black Vertisols (Black Earths) in areas of less frequent flooding.

1.5   Hydrogeology

Broughton [3] studied the hydrogeology of the Liverpool Plains, and produced a hydrogeological map of the area (Broughton [4]). Rising water levels in the alluvial deposits were reported in this work based upon an analysis of current (1992/93) water levels and water levels in previous years. The development of dryland salinity was identified as a major risk to agricultural productivity on the plains if these water level rises continued unchecked. Timms [18] has updated some of the initial work by Broughton and reports that the area affected by shallow groundwaters has decreased between 1992 and 1997, and that there is a patchy and localised distribution of shallow groundwater.

Water levels in piezometers in the northern part of Yarramanbah Creek are close to ground level and have salinity levels approaching that of sea water, especially at the southern end of Cattle Lane. It was anticipated that these saline waters could be economically mapped using geophysical techniques, and the data then used to assist agricultural management in this part of the Plains.

Acworth and Jankowski [1] have reported that similar bulk electrical conductivity anomalies at Breeza, further north along the Mooki River, are associated with salty water contained in the clays rather than a regionally rising salty water table. If this is the case, there may be significantly different land management implications for these areas, which should concentrate on managing the areas affected by salty clays rather than the more regional strategy which concentrates on the management of rising water tables.

The current project seeks to establish the reasons for the bulk electrical conductivity anomalies at Yarramanbah / Pump Station Creek.

Chapter 2

INVESTIGATION METHODS

2.1 Program Organisation

The survey area was selected based upon the extensive data set which has been compiled for this catchment by DLWC. Part of this data set, acquired during 1994, is shown in Figure 2.1. A sub-area was selected for detailed work, with the objective of establishing the physio-chemical properties of the alluvial clays in an area where a strong contrast in σ_a had been established. The EM-31 data for this area was resurveyed in April, 1997.

Four borehole sites were selected. Borehole N1 was drilled to sample a zone of high σ_a. Boreholes N3 and N4 were drilled to establish the characteristics of the low σ_a ground, and borehole N2 was carefully selected to sample conditions on the boundary of the anomaly.

2.2 EM-31 and EM-38 Surveys

The EM-31 was mounted in vertical dipole mode on the back of a QUADCYCLE which had been equipped with a Global Positioning System (GPS). Survey lines were run at 50 m intervals with data points recorded approximately every 5 m. This configuration allows the rapid collection of large amounts of data. The QUADCYCLE is particularly suited to the flat open fields of the Liverpool Plains.

Detailed grids of measurements with the EM-38 were carried out around each borehole to measure the variability of bulk electrical conductivity around each bore at shallow depth. The EM-38 in vertical mode has an approximate depth of penetration of 1.5 m. In horizontal mode the depth of penetration is reduced to 0.75 m.

2.3 Electrical Image Acquisition

A multi-core cable with 25 electrodes was connected to a switch box and readings of resistance made using an ABEM SAS 300B resistance meter. A schematic of the measurement technique is shown in Figure 2.2 after Griffiths & Barker [8].

Interpretation of the images was carried out using a program developed by Loke and Barker [10], [11]. The sub-surface is divided into blocks associated with each of the measurement points indicated in Figure 2.2.
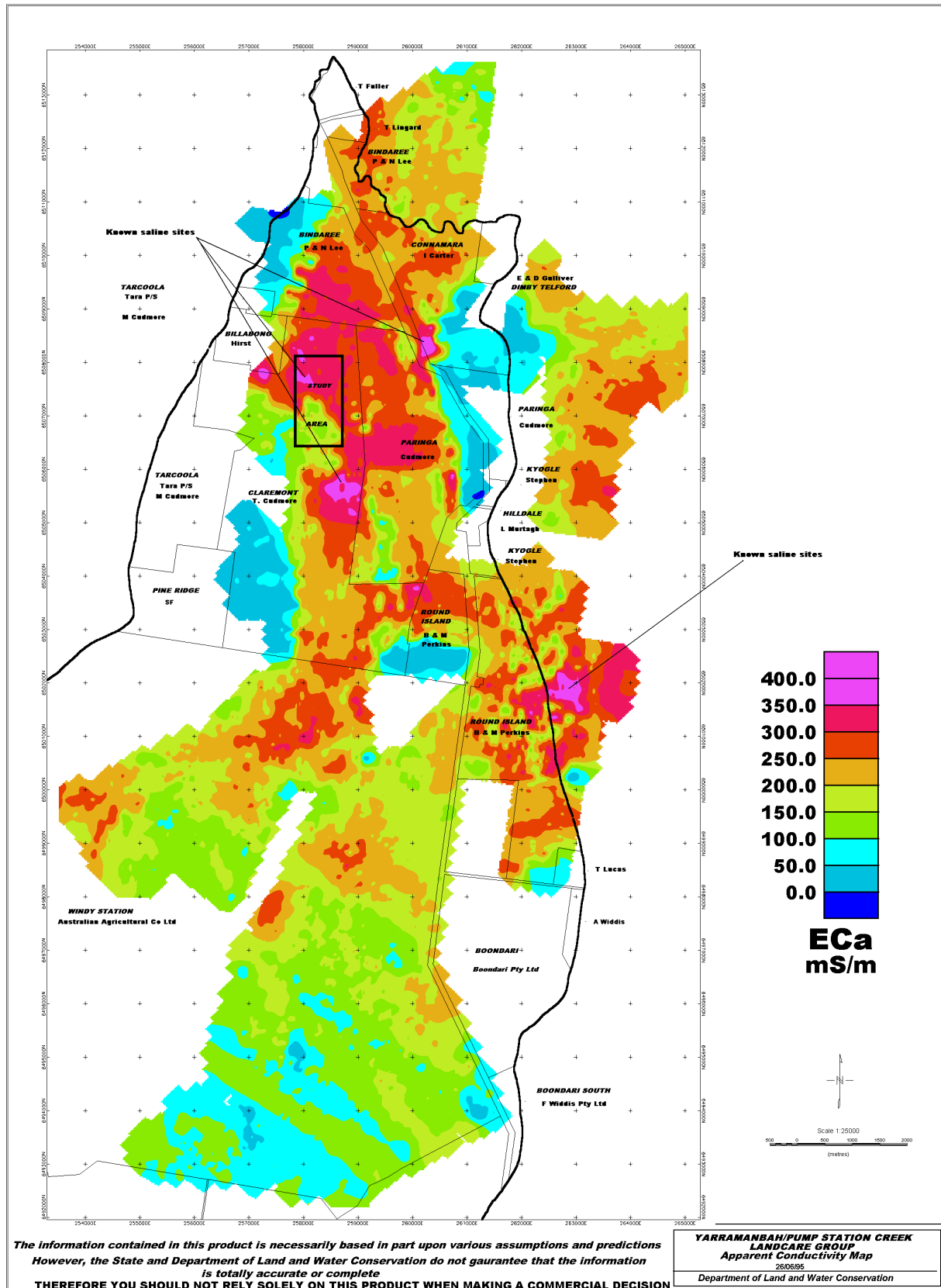
Figure 2.1: EM-31 Data for the Yarramanbah / Pump Station Creek Landcare Group
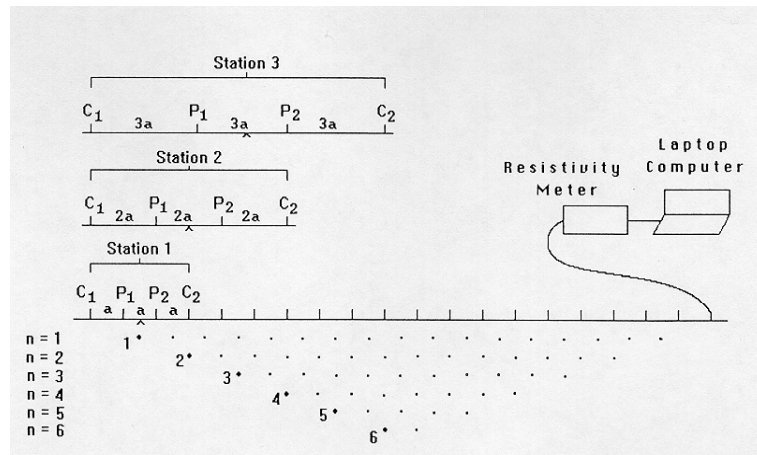
Figure 2.2: Measurement system for electrical image data acquisition
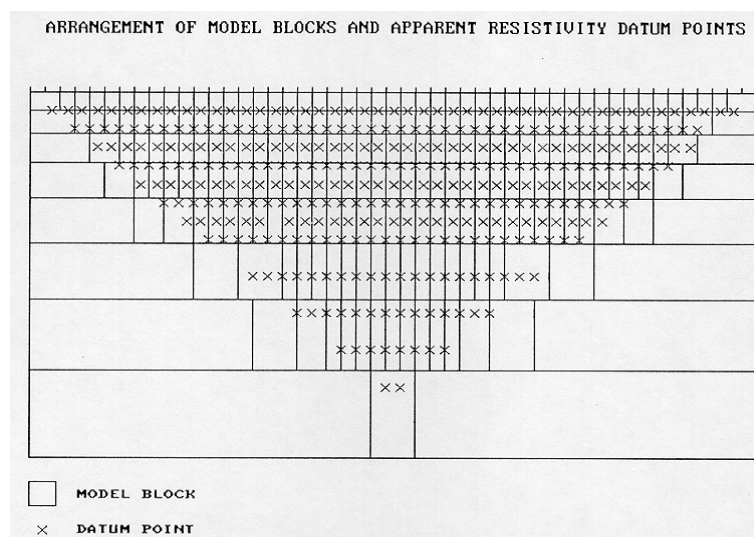
Figure 2.3: Arrangement of model blocks and apparent conductivity datum points

A 2-D finite difference modeling package is then used to fit the field data to a theoretical model. The end result is that each of the blocks shown in Figure 2.3 is assigned a value of electrical conductivity valid within a specified volume of material around each measurement point.

2.4 Drilling and Coring

The bores were installed using a drilling rig equipped with hollow-stem augers. The bores were all cored. To obtain good quality, minimally disturbed core samples in the clay, an HQ triple tube (HQ3) coring system was modified to recover core from the interior of the 250 mm hollow flight augers using a wire-line system. The inner sample barrel from the HQ3 drilling system was adapted to engage a casing advance latch mechanism installed in the lead auger. The inner barrel fitted inside and protruded through the bottom cutting face of the lead auger. The latch mechanism located the sample barrel inside the lead auger and enabled the sample barrel to remain free from the rotation of the auger. This was achieved by use of a thrust bearing and ball race incorporated into the latch mechanism. The latch mechanism allowed for easy recovery of the 1.5 m long sample barrel via the use of standard wire-line recovery techniques.

The sample barrel was lined with a clear PET liner and the core was acquired inside the liner. To prevent cross contamination, the use of water was limited to core barrel withdrawal. The sample barrel containing the liner and core were recovered to the surface using the wire line. The core and liner were then expelled from the core barrel and the ends of the PET liner capped with PET caps and sealed with water-proof tape. This method allowed core to be recovered from all boreholes to depth.

Each of the bores was drilled dry. Water seeped into the bores within 24 hours as the result of the pressure differential between the moisture held in the clay by surface tension and the atmospheric pressure in the hole. Water levels in these piezometers represent the combined effects of water pressure due to the high water content in the clays and a partial response due to the weight of the overlying clay (overburden pressure) as described by Jury et al. [9]. They do not represent a true water table condition.

The bores were completed as 50 mm PVC piezometers with a medium sand pack filling the annulus between the 250 mm diameter hole left by the auger and the 60 mm outer diameter of the PVC. The top of the hole was sealed with a cement grout and a monument installed to protect the PVC casing from farming activities and UV radiation from the sun. The drilling was carried out in April, 1997, by Reynolds Drilling and was supervised by Mark Groskops of the WRL.

2.5   EM-39 Borehole Logging

A GEONICS EM-39 was used to log the four boreholes. The EM-39 has a sonde which measures apparent σ_a as a function of depth using an electromagnetic induction technique which is based on exactly the same physical principles as the EM-31. The σ_b can be measured through the PVC casing using this technique and is also not affected by the conductivity of the fluid in the bore. The sonde is designed to give a measure of σ_a in the formation at approximately 500 mm from the bore. A review of the application of this equipment to ground-water studies is given by Taylor et al. [17], and details of the theoretical basis behind the EM-39 are given by McNeill [12].

The GEONICS equipment also has a sonde which is designed to measure the gamma-ray activity of the soil. Gamma rays are produced by the spontaneous decay of unstable isotopes in the soil. Naturally occurring isotopes are Potassium-40, Uranium-238, and Thorium-232. Potassium is abundant in some feldspar and micas which decompose to clay. Uranium and thorium are concentrated in clay by the processes of adsorption and ion exchange. A log of gamma-ray activity is therefore often used as a log which indicates clay content.

Field measurements of bulk electrical conductivity and gamma-ray activity were made in May, 1997.

2.6   Core Analyses

The cores were delivered from the field to the WRL and stored in their PET liners prior to analysis. The first stage of analysis involved splitting the cores into 100 mm sub-cores and re-capping with PET caps. The cores were individually described and labeled at this stage.

The cores were split into two groups, with alternate core sub-samples sent to the Gunnedah Research Station Laboratory for preparation and analysis of 1:5 extracts, grain-size determination and cation exchange capacity determination. The remaining cores were held at the WRL for X-Ray Diffraction measurements, bulk electrical property determination, and for the measurement of hydraulic conductivity.

Attention was focused on core from Borehole N2 as it passed through the edge of a major anomaly of interest. Core from Borehole N3 and Borehole N4 was considered to be very similar and therefore the N3 core was not submitted for analysis.

2.6.1 Particle Size Analysis

This was determined after $50\,\mathrm{g}$ of soil had been shaken for 16 hours in $200\,\mathrm{mls}$ of 12.5% sodium poly-metaphosphate/sodium carbonate solution. After shaking, periodic hydrometer readings were taken to determine size fractions in suspension at set times. After 7.75 hours, the suspension is sieved for the determination of sand fractions (SAA [14]).

2.6.2 Moisture Content

The core sample was opened and a sub-sample taken for determination of the field moisture content. The remaining sample was allowed to dry at $40\,^\circ\mathrm{C}$ until dry enough to crush. The moisture content was then determined gravimetrically, and represents the moisture held in the sample which could be said to be readily lost by drying.

2.6.3 Field Moisture Content

A subsample of the core was taken and weighed. Field moisture content was determined on soil crushed to $< 2.0\,\mathrm{mm}$ and was a measure of the weight loss after drying for 16 hours in a fan forced oven at $105\,^\circ\mathrm{C}$. This enabled all results to be corrected for moisture content, although moisture correction was not applied to electrical conductivity results (Standards Association of Australia 1977 - AS 1289 [15]).

2.6.4 Porosity Determination

Sample porosity was determined for a small set of samples from Bores N1, N2, and N3 by making measurements of sample density and moisture content.

The porosity can be determined from Equation 2.1, as the product of the sample density and the moisture content:

$$\phi = \frac{V_l}{V_t} = \frac{M_t}{V_t} \times \frac{V_l}{M_t} \tag{2.1}$$

where:

ϕ is the porosity,

V_l Volume of liquid,

V_t Total volume,

M_t Total mass of the sample,

The sample density was determined by taking a mini-core of a sub-sample of the clay using a stainless steel corer. The length and diameter of the mini-core were determined using calipers and the weight measured on a balance. The density was then:

$$\rho = \frac{M_t}{V_t} \tag{2.2}$$

Measurements from at least two mini-cores were taken from each sub-core to estimate the error in measurement. Moisture content was determined on a sample of approximately $5\,\mathrm{g}$ of homogenised sample placed in a pre-weighed porcelain dish and oven-dried at $105\,^\circ\mathrm{C}$ for 24 hours. The samples were then removed and placed in a dessicator to cool and then deweighed. The samples were then dried for a further
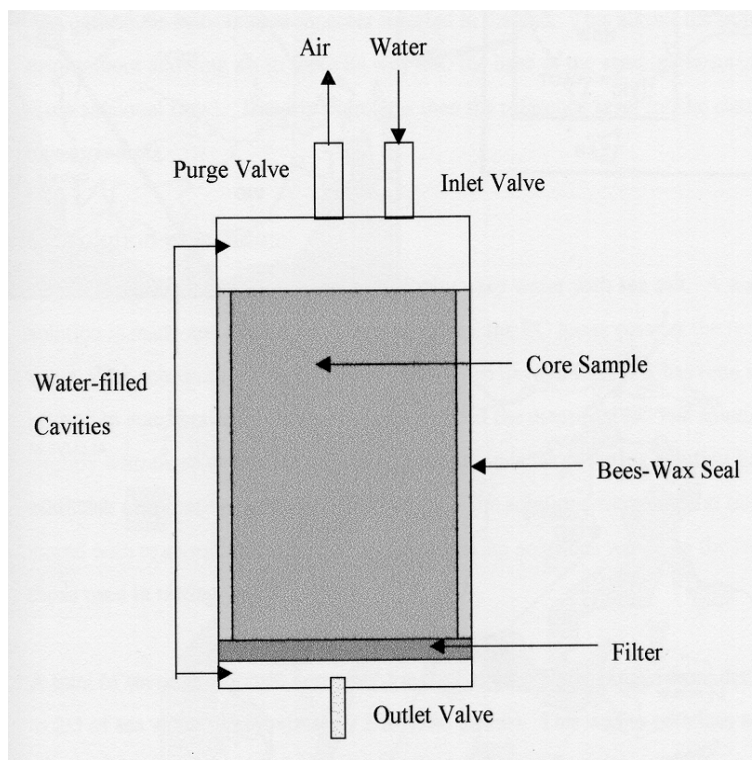
Figure 2.4: Schematic of the core holder for falling head testing

24 hours to check for completeness of drying. In all cases there was no further weight loss. The mass of liquid M_l, determined by difference after drying, was equated to the volume of liquid V_l in Equation 2.1 as the density of water was approximated to 1.0.

2.6.5 Hydraulic Conductivity

A 10 m falling-head permeameter was used to establish the hydraulic conductivity of selected clay cores to a range of fluid electrical conductivities. This work is described in detail by Crawford [5]. A schematic of the core testing apparatus is shown in Figure 2.4 after Crawford [5].

The samples were potted into clear perspex containers using beeswax. This approach ensured that leaks around the seal could be detected during testing. The samples were saturated for varying time periods prior to testing.

The effect of different water chemistries on the hydraulic conductivity was established by saturating the samples with waters of different fluid electrical conductivity (EC). The EC was established by adding salt to water.

2.6.6 Geophysical Measurements

Dr Emmerson of SYSTEMS EXPLORATION (NSW) Pty Ltd carried out the geophysical measurements on selected core sub-samples.

Frequency domain complex resistivity measurements were made in the laboratory using a Solarton 1250 Frequency Analyser with measurement interval of 3 steps/decade. The sample was placed in a four

electrode water bath with an energising sine wave of amplitude $100\,\mathrm{mV}$ and a current of approximately $1\,\mathrm{mA}$. The water in the end baths had a resistivity of $1.3\,\mathrm{ohm}\ \mathrm{m}$ at $13\,^{\circ}\mathrm{C}$. Measurements were integrated over 20 cycles.

Results are presented for a single frequency of $1\,\mathrm{kHz}$.

Measurements of apparent density and the primary wave ultrasonic velocity at $500\,\mathrm{kHz}$ were also measured under a $5\,\mathrm{kN}$ uniaxial load.

2.6.7   X-Ray diffraction Measurement

Dr DeLeon of ROCKMIN LABORATORY carried out the X-Ray diffraction measurements on selected core samples. Sub-samples of between $5\,\mathrm{g}$ and $10\,\mathrm{g}$ were taken from each of core, dried to $100\,^{\circ}\mathrm{C}$, pulverised and analysed as a bulk sample by X-Ray diffraction using Co radiation. The bulk samples were slightly compressed into a holder and were randomly orientated for subsequent X-ray analysis.

A typical clay fraction $(<\ 2\mu m)$ of the sample was prepared using sedimentation and centrifugation techniques. This was deposited onto a small unglazed porcelain tile such that predominantly basal-oriented clay particles were presented for X-ray analysis.

The clay specimens were analysed on two XRD instruments using Co and Cu radiation. The following spectra were recordec:

- as separated,

- expanded with ethylene glycol,

- heated to $250\,^{\circ}\mathrm{C}$,

- heated to $350\,^{\circ}\mathrm{C}$, and

- heated to $600\,^{\circ}\mathrm{C}$.

These treatments served to differentiate between smectite and chlorite minerals.

2.7   Soil Water Extracts

2.7.1   Preparation of Soil Water Extract (1:5)

A volume of deionised water was added to a known mass of soil such that there was $5\,\mathrm{mls}$ water for each gram of soil. The solution was then shaken for an hour at 15 r.p.m.

2.7.2   Electrical Conductivity σ_w

Electrical conductivity was used to estimate the concentration of soluble salts in the soil. The determination was made on a 1:5 soil water solution after a period of settling. A conductivity cell with internal temperature compensation was used, with the result expressed in dSm^{-1}

2.7.3   pH(water)

pH was determined on a 1:5 soil water suspension using a combination electrode and a digital pH meter. The measurement was made while the solution was being stirred (Rayment and Higginson [7]).

pH in Calcium Chloride is measured after adding calcium chloride to the 1:5 soil/water suspension to produce a $CaCl_2$ concentration of 0.01 M. The measurement is made after settling, and with out stirring (Rayment and Higginson [7]).

2.7.4   Chloride

Chloride was measured on a 1:5 soil water solution. The solution was titrated with 0.05 M $AgNO_3$ to a potentiometric end point. The titration is conducted using an auto-titrator after the method described by Metson [13].

2.7.5   Soluble Carbonate

Soluble carbonate was determined on a 1:5 soil water extract. CO_3 and HCO_3 were determined by titration with 0.05 M H_2SO_4 to pH end points of 8.2 and 4.5 respectively using an auto-titrator.

2.7.6   Soluble Sulphate

A 1:5 water solution was used for the measurement. Under controlled conditions SO_4 was precipitated by reaction with $BaCl_2 2.2H_2O$. The turbidity which results was measured with a double beam spectrophotometer at a wavelength of 420 nm (Metson [13]).

2.7.7   Soluble Cations

Cations were extracted in a 1:5 soil/water solution and then measured using Atomic Absorption Spectrophotometry (AAS) (Emmel et al. [6]).

2.7.8   Cation Exchange Determination

A single saturation of the soil sample with 0.01 M silver-thiourea solution was prepared and the CEC and exchangeable cations measured by analysing the extract for silver, calcium, magnesium, sodium and potassium. Measurement was made with AAS.

2.7.9   Exchangeable Cations

Exchangeable cations were determined after alcohol and aqueous glycerol washing to remove soluble bases. The soils were equilibrated with 1 M ammonium chloride at pH 7.0 for 1 hour with mechanical shaking at a soil/solution ratio of 1:20. The suspensions were clarified and analysed for exchangeable bases. Principal exchangeable bases are measured using AAS. Effective cation exchange capacity was then determined by summing the exchangeable bases [7].

2.8 Hydrochemistry

2.8.1 Field Measurement

Groundwater samples were taken from the shallow piezometers using a submersible bilge pump (AMA-ZON). All piezometers were pumped until stable field chemistry was obtained. This procedure ensured that representative groundwater samples were obtained.

Field measurements consisted of all unstable parameters and included temperature, fluid electrical conductivity (EC), pH, redox potential (Eh), dissolved oxygen (DO), alkalinity and carbon dioxide. Water samples for chemical analyses of major ions were filtered in the field using a 0.45μm filter (Millipore cellulose acetate membrane). Measurements of Carbonate, Bicarbonate, Iron^{2+} and Sulphur^{2-}, were carried out in the field using the UNSW Groundwater Centre Mobile Laboratory.

2.8.2 Laboratory Determination

Samples for cation determination were preserved in the field by acidifying using nitric acid and analysed in the laboratory using atomic absorption spectrometry (AAS) and inductively coupled plasma atomic emission spectroscopy (ICP-AES). Chloride was determined by an argentometric method and sulphate (as total sulphur) by ICP.

Chapter 3

RESULTS

3.1 EM-31 Survey

The field area in Yarramanbah / Pump Station Creek was selected after inspection of extensive EM-31 surveys carried out for the local Landcare group. High values of apparent σ_a were shown by this work in the area at the bottom of Yarraminbah Creek, upstream of the confluence with Warrah Creek. A further EM-31 survey was carried out to detail the edge of this larger anomaly, so that bores could be located to sample both the high apparent σ_a values, intermediate values at the edge of the anomaly and the low apparent σ_a areas to the south.

The results from the EM-31 survey were plotted and presented as a contour map, which is shown in Figure 3.1. T test the effect of local variability in the EM-31 data, additional detailed surveys were carried out in the immediate vicinity of Bore N1 using an EM-31 in both horizontal and vertical mode. Te near surface variability was investigated using an EM-38 in both horizontal and vertical mode with measurements taken on a 5 m grid. The results of these surveys are shown in Figure 3.2 and Figure 3.3 for the EM-31 and in Figure 3.4 and Figure 3.5 for the EM-38, at bore N1. The data for bore N4 are shown in in Figure 3.6 and Figure 3.7 for the EM-31 and in Figure 3.8 and Figure 3.9 for the EM-38, respectively.

3.2 Electrical Image Data

An electrical image was orientated along the line of the bores N1 and N4. The location of the image line is shown in Figure 3.1.

The interpreted data is shown in Figure 3.10.

3.3 Drilling

Four bores were successfully established on the Claremont property. The bores were drilled in reverse order (N4 to N1). Bores N4, N3, and N2 were completely cored with little loss of material. The core logs are in Appendix A. The bores were completed as 50 mm piezometers to a depth of approximately 11 m. The piezometer intake was 1.5 m in length and placed at the base of the piezometer.
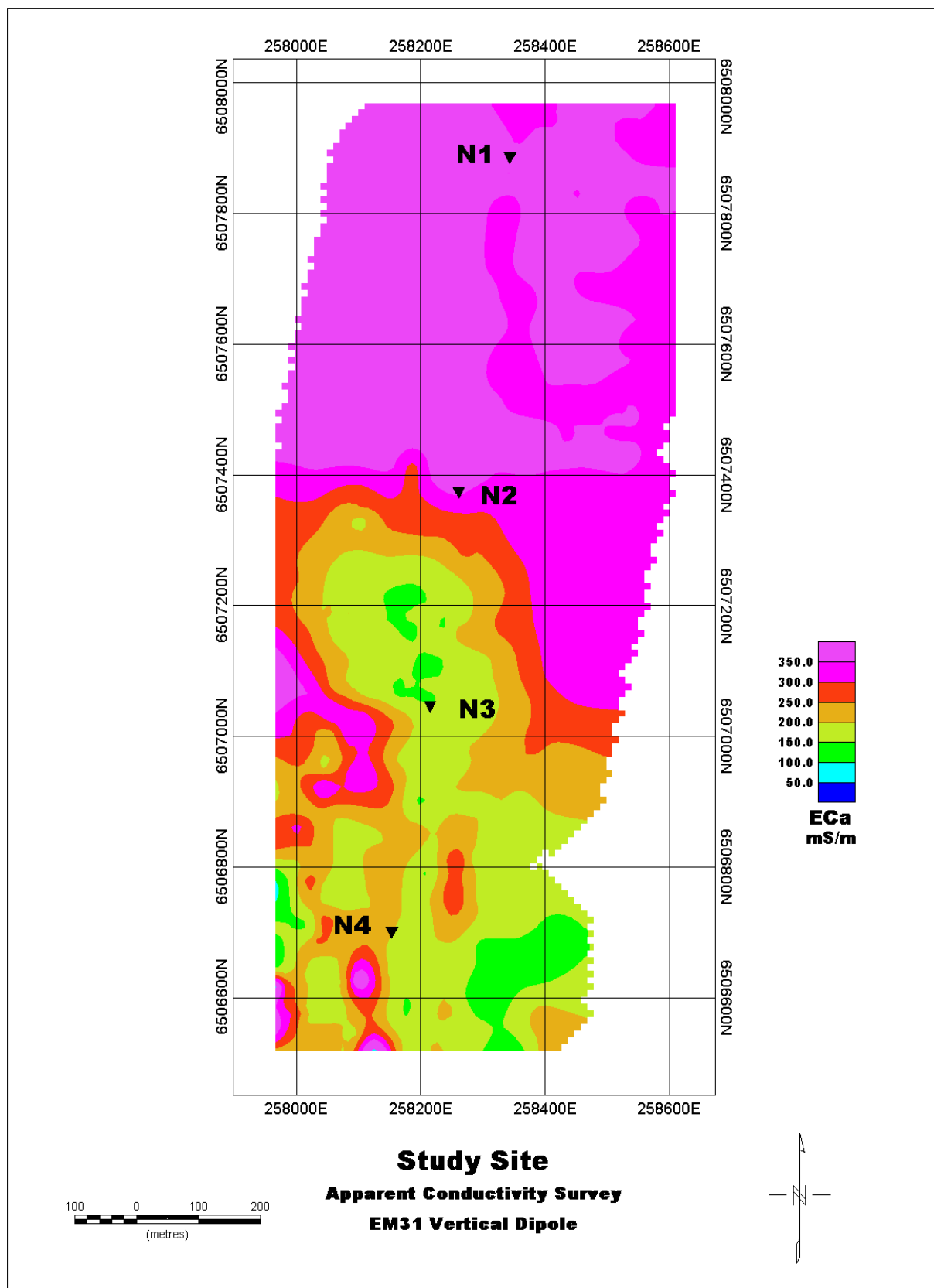
Figure 3.1: EM-31 Data for the Study Survey - Locations of Bores N1 - N4 shown
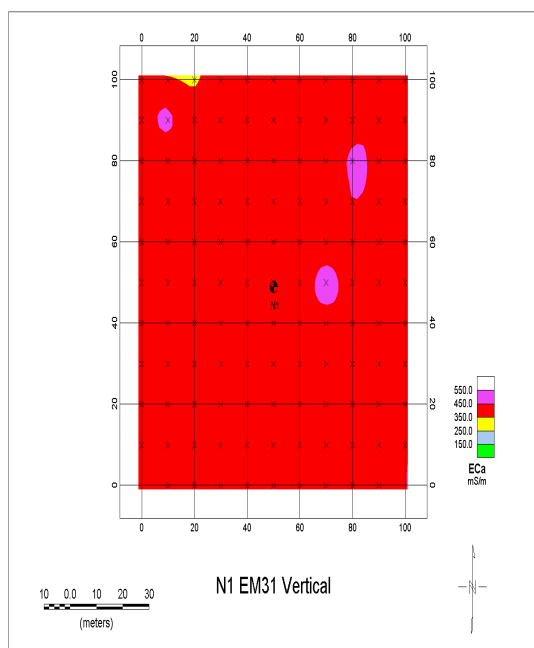
Figure 3.2: EM-31 Vertical Mode at Bore N1 (≈6 m penetration)
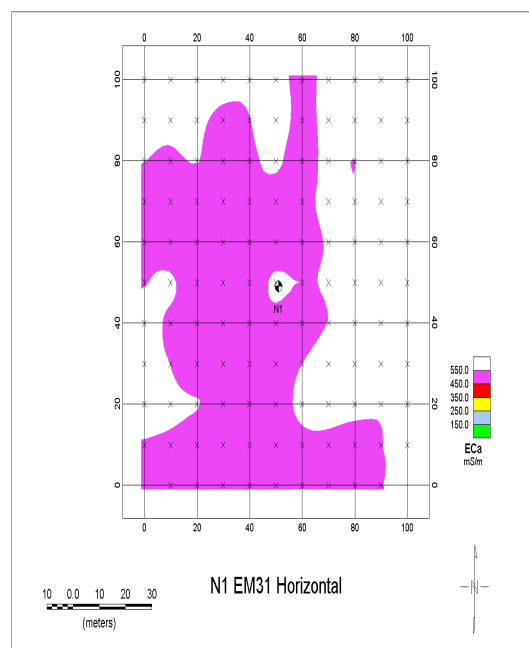
Figure 3.3: EM-31 Horizontal Mode at Bore N1 (≈3 m penetration)
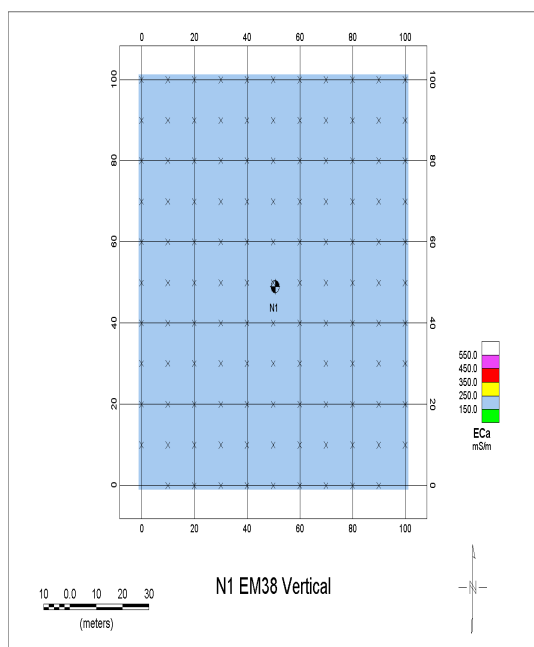
Figure 3.4: EM-38 Vertical Mode at Bore N1 (≈1.5 m penetration)
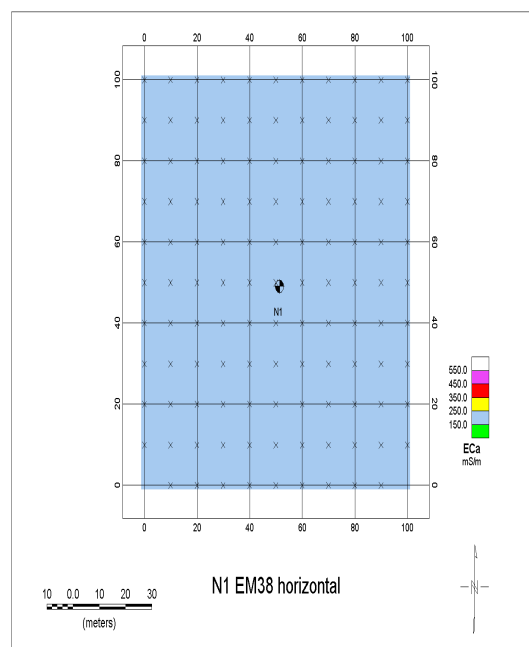
Figure 3.5: EM-38 Horizontal Mode at Bore N1 (≈0.75 m penetration)
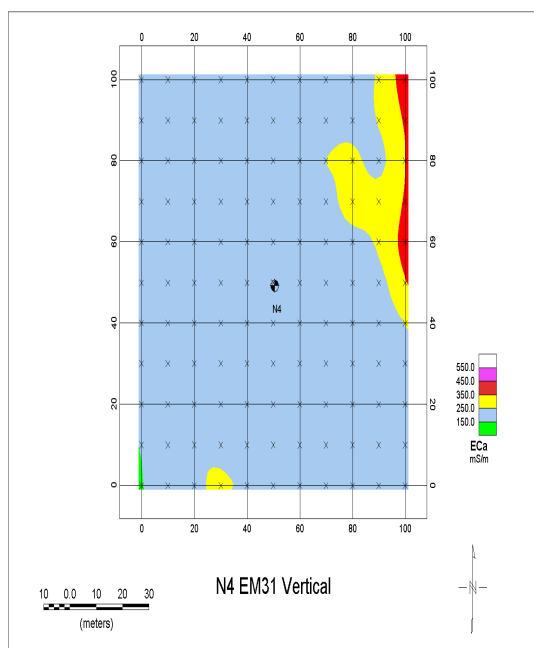
Figure 3.6: EM-31 Vertical Mode at Bore N4 (≈ 6 m penetration)
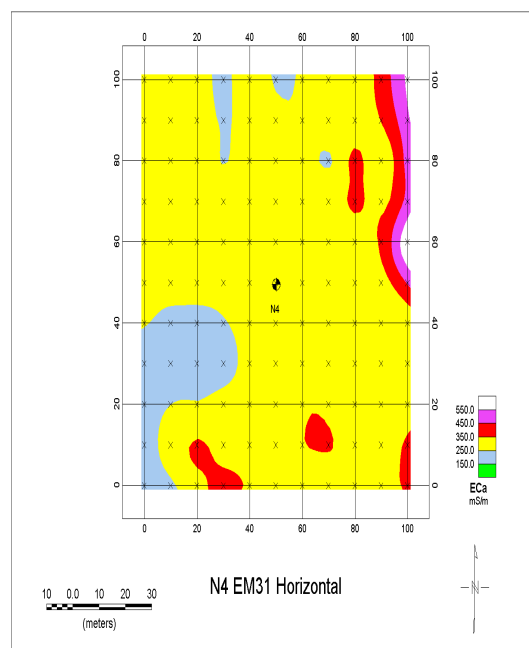
Figure 3.7: EM-31 Horizontal Mode at Bore N4 (≈ 3 m penetration)
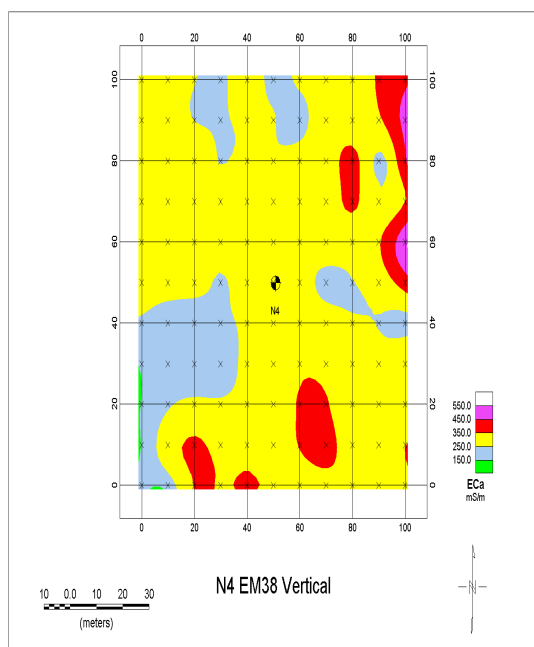
Figure 3.8: EM-38 Vertical Mode at Bore N4 (≈ 1.5 m penetration)
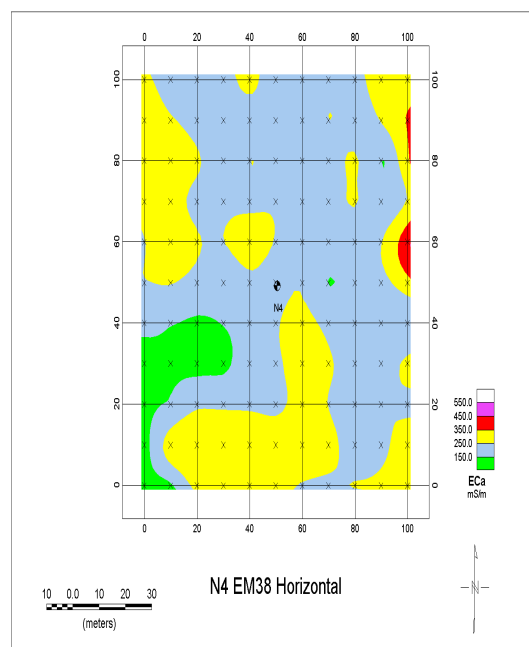
Figure 3.9: EM-38 Horizontal Mode at Bore N4 (≈ 0.75 m penetration)
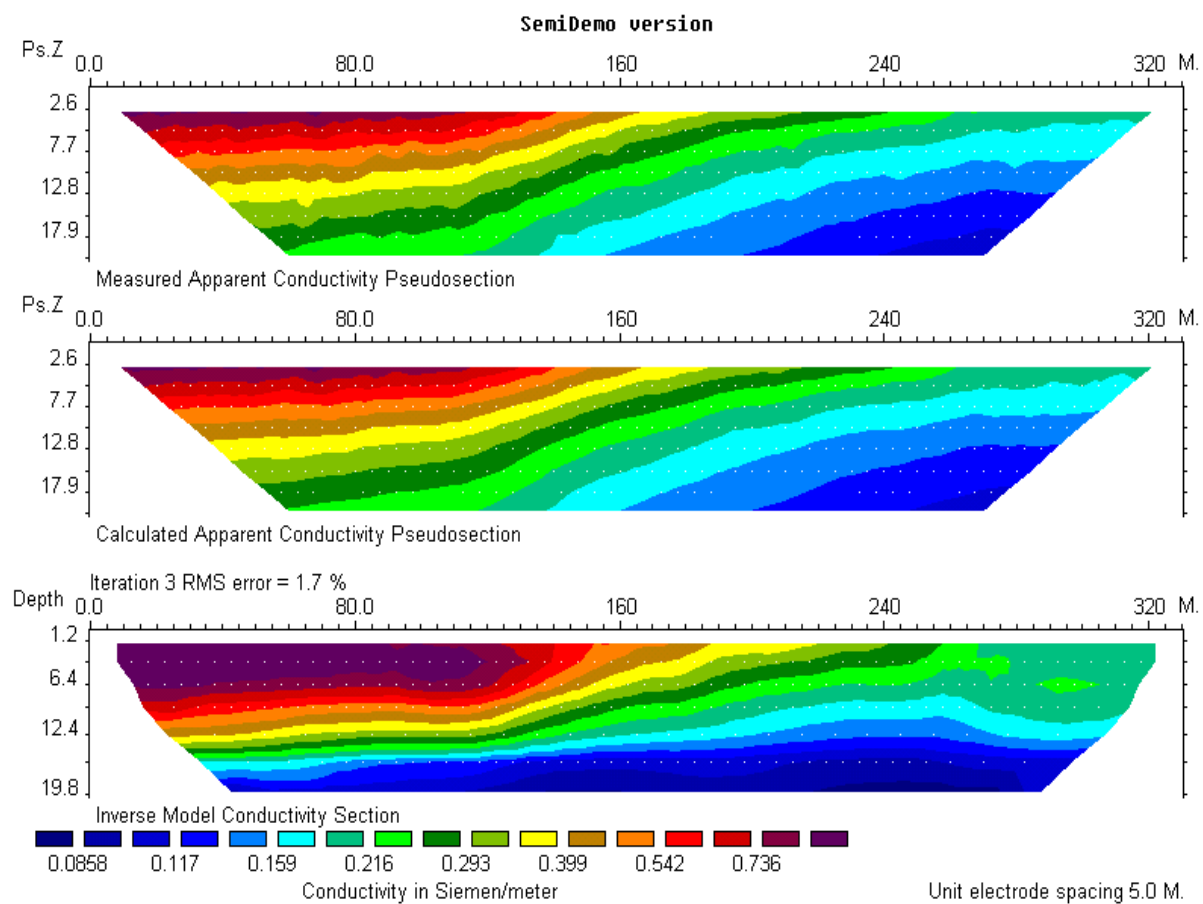
Figure 3.10: Image line through the edge of the EM-31 anomaly (Bore N2 at 120 m)
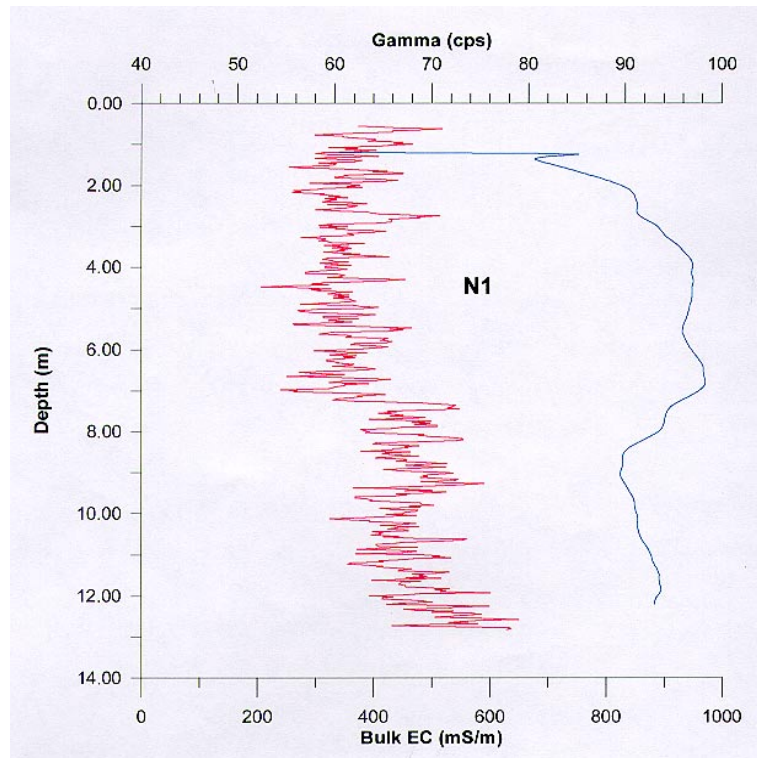
Figure 3.11: σ_b and Gamma Logs for Borehole N1

Some core loss occurred in Bore N1 when highly swelling clays were encountered. It was intended initially to core this bore to the same depth as the first three and to then drill on to 20 m depth to install a deeper piezometer. In the event, drilling became very difficult below 13 m depth and the piezometer was terminated at that depth. The piezometer completion details are shown in Table 3.1. Water level data was measured on 6 April, 1998.

Table 3.1: Piezometer Completion Details

Piezometer Number	Height of PVC above ground (m)	Depth of Piezometer (m bgl)	Screen Section (m bgl)	Standing Water Level (m bgl)
N1	0.60	12.84	11.32 - 12.82	0.25
N2	0.63	11.71	10.19 - 11.69	0.24
N3	0.52	11.66	10.61 - 11.64	0.19
N4	0.55	11.69	10.17 - 11.67	0.16

3.4 EM-39 Borehole Logging

The results of the EM-39 logging are shown in Figures 3.11 to 3.14 for boreholes N1 to N4 respectively.
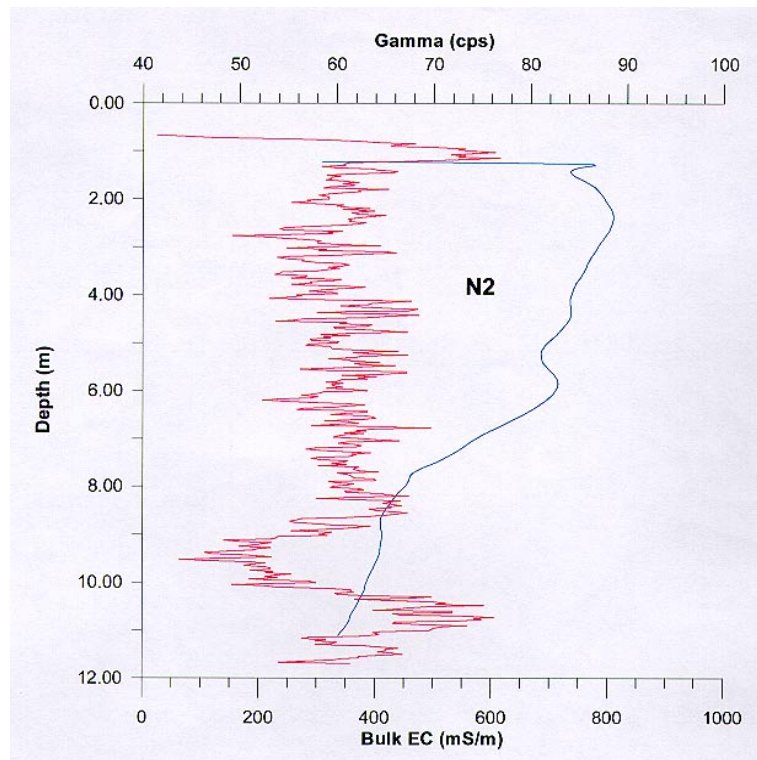
Figure 3.12: σ_b and Gamma Logs for Borehole N2
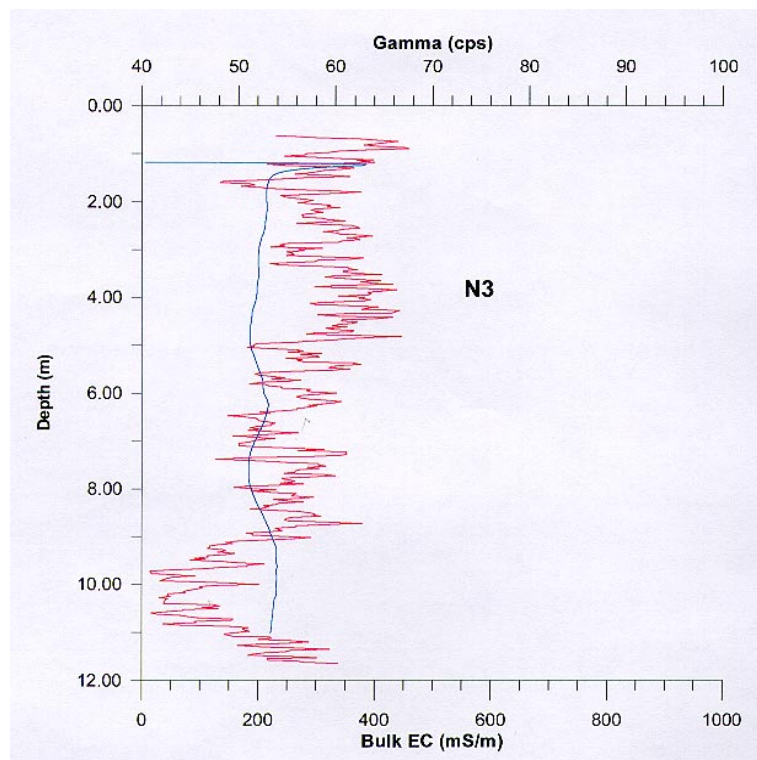
Figure 3.13: σ_b and Gamma Logs for Borehole N3
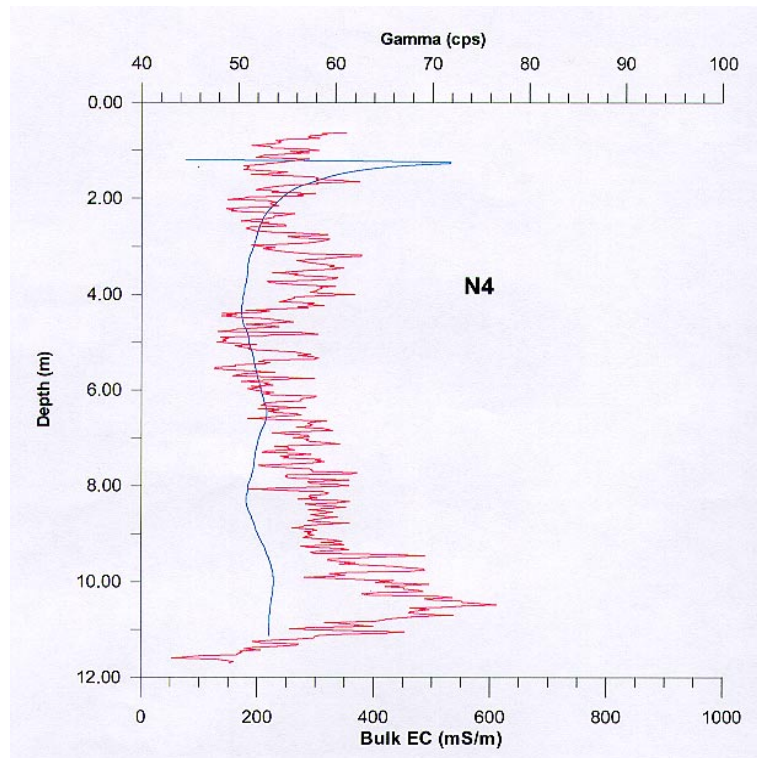
Figure 3.14: σ_b and Gamma Logs for Borehole N4

3.5 Core Analyses

Analysis of the borehole geophysics data indicated that both Bores N3 and N4 lay off the high apparent σ_a anomaly. For this reason, cores from Bore N3 were not included in the core analysis program. Furthermore, as Bore N2 passed from high apparent σ_a values at the top to low apparent σ_a values at the base, which seemed to be transitional between conditions at Bore N1 and N3 respectively, attention was concentrated on determining the reasons for this change in this borehole. Visual inspection of the cores (presented in the Appendix) did not give any indication of a change in bulk properties.

3.5.1 Moisture Content & Grain Size Determinations

Moisture content and grain size determinations were carried at the Gunnedah Research Centre.

The results for bores N1, N2 and N4 are presented in Table 3.2, Table 3.3 and Table 3.4 respectively.

Table 3.2: Grain Size Measurements for N1 Samples

Sample ID Method	Depth to Sample Base (m)	Moisture Content % P1A/1	Field Moisture % N.S.	Clay % P7B/3	Silt % P7B/3	Fine Sand % P7B/3	Coarse Sand % P7B/3	Gravel % P7B/3
N1-C1.2	0.60	9.34	39.78	65.5	24.4	8.7	1.4	0.0
N1-C2.4	1.10	8.54	40.48	53.0	36.3	10.0	0.7	0.0
N1-C3.3	1.55	8.96	40.39	62.0	34.8	2.5	0.8	0.0
N1-C3.7	1.95	9.61	40.33	55.7	38.1	5.2	0.9	0.0
N1-C4.3	2.30	9.24	40.16	57.8	33.2	8.2	0.8	0.0
N1-C4.7	2.70	8.71	40.49	61.8	32.3	4.9	0.9	0.0
N1-C5.2	3.10	10.31	40.28	60.0	34.3	4.0	1.7	0.0
N1-C6.1	3.90	10.75	40.66	51.9	39.2	8.0	0.9	0.0
N1-C6.5	4.30	11.93	40.83	63.7	32.1	3.8	0.4	0.0
N1-C6.9	4.70	12.58	40.24	61.7	30.8	6.9	0.5	0.0
N1-C7.4	5.15	10.55	40.43	69.6	16.6	13.0	0.8	0.0
N1-C7.6	5.35	10.10	40.12	68.3	28.2	3.0	0.6	0.0
N1-C7.8	5.55	11.14	40.51	62.0	33.1	4.6	0.3	0.0
N1-C8.3	6.10	11.00	40.42	60.9	35.2	3.6	0.3	0.0
N1-C8.7	6.50	9.92	40.42	60.3	32.6	6.7	0.4	0.0
N1-C9.2	6.88	9.85	40.56	54.8	33.3	11.6	0.4	0.0
N1-C10.1	7.55	10.46	40.34	46.2	37.5	12.8	3.5	0.0
N1-C11.1	7.80	10.51	40.76	48.4	44.9	6.4	0.3	0.0
N1-C11.3	8.00	13.47	40.45	52.0	38.9	8.6	0.4	0.0
N1-C12.2	8.70	9.93	39.97	61.4	32.7	5.5	0.4	0.0
N1-C12.6	9.10	11.30	40.22	65.6	28.4	5.7	0.3	0.0

Table 3.3: Grain Size Measurements for N2 Samples

Sample ID Method	Depth to Sample Base (m)	Moisture Content % P1A/1	Field Moisture % N.S.	Clay % P7B/3	Silt % P7B/3	Fine Sand % P7B/3	Coarse Sand % P7B/3	Gravel % P7B/3
N2-C1.2	0.55	12.47	59.89	61.3	20.5	17.6	0.6	0.0
N2-C1.4	0.75	11.80	61.35	71.1	19.8	7.8	1.4	0.0
N2-C2.2	1.25	11.30	59.22	74.2	16.2	8.7	0.9	0.0
N2-C2.4	1.45	10.82	59.33	75.0	17.5	6.8	0.7	0.0
N2-C2.6	1.65	9.96	58.82	73.3	19.7	6.4	0.6	0.0
N2-C3.2	1.90	10.64	62.51	73.8	18.6	7.4	0.2	0.0
N2-C3.4	2.10	9.97	53.60	68.8	24.2	6.4	0.6	0.0
N2-C3.6	2.30	9.04	52.03	64.9	27.3	6.9	0.9	0.0
N2-C3.8	2.50	9.93	55.75	64.3	28.6	6.2	0.8	0.0
N2-C4.2	2.70	9.77	57.85	66.5	25.1	6.7	1.7	0.0
N2-C4.4	2.90	9.36	57.78	61.8	27.1	10.6	0.6	0.0
N2-C4.6	3.10	7.70	48.48	53.3	29.6	15.8	1.3	0.0
N2-C4.8	3.30	7.67	31.26	56.5	24.0	16.3	3.2	0.0
N2-C5.2	3.75	8.08	51.21	52.3	29.8	17.4	0.5	0.0
N2-C5.4	3.95	8.68	51.62	54.8	25.3	19.7	0.2	0.0
N2-C5.6	4.15	8.87	51.42	52.7	30.0	16.9	0.4	0.0
								continued on next page

Table 3.3: Grain Size Measurements for N2 Samples

Sample ID Method	Depth to Sample Base (m)	Moisture Content % P1A/1	Field Moisture % N.S.	Clay % P7B/3	Silt % P7B/3	Fine Sand % P7B/3	Coarse Sand % P7B/3	Gravel % P7B/3
N2-C6.1	4.45	8.60	52.19	74.6	12.5	9.4	3.5	0.0
N2-C6.3	4.65	8.79	46.00	77.0	15.0	5.4	2.6	0.0
N2-C6.5	4.85	8.78	57.07	72.5	25.5	1.8	0.3	0.0
N2-C6.7	5.05	9.16	55.43	73.8	24.5	1.4	0.3	0.0
N2-C7.2	5.40	9.86	58.97	75.5	23.5	0.7	0.3	0.0
N2-C7.4	5.60	9.59	55.36	77.6	21.1	0.9	0.4	0.0
N2-C7.6	5.80	10.16	56.83	76.9	22.3	0.5	0.3	0.0
N2-C7.8	6.00	10.80	63.63	75.9	23.6	0.2	0.4	0.0
N2-C8.1	6.20	10.25	57.20	75.8	23.5	0.5	0.2	0.0
N2-C8.3	6.40	10.60	61.31	73.7	23.4	2.6	0.4	0.0
N2-C8.5	6.60	10.02	57.20	71.0	23.1	5.6	0.3	0.0
N2-C8.7	6.80	9.44	58.26	70.7	21.9	6.8	0.7	0.0
N2-C8.9	7.00	10.17	57.47	71.2	22.0	6.4	0.5	0.0
N2-C9.2	7.25	10.63	60.07	67.0	26.6	6.1	0.3	0.0
N2-C9.4	7.45	9.77	55.20	66.5	26.3	6.7	0.5	0.0
N2-C9.6	7.65	9.76	54.07	66.5	26.3	6.7	0.5	0.0
N2-C9.8	7.85	9.70	56.21	65.3	27.5	7.0	0.3	0.0
N2-C10.1	7.95	9.16	51.91	62.8	24.8	12.1	0.3	0.0
N2-C10.3	8.15	10.59	57.59	71.0	21.3	7.2	0.5	0.0
N2-C10.5	8.35	10.84	53.58	75.0	17.5	7.0	0.5	0.0
N2-C10.7	8.55	11.07	64.21	76.3	18.7	4.5	0.5	0.0
N2-C10.9	8.75	11.86	65.17	76.9	18.9	3.8	0.5	0.0
N2-C11.2	8.95	11.39	64.66	77.8	17.6	4.1	0.6	0.0
N2-C11.4	9.15	10.61	58.47	74.8	18.7	6.0	0.5	0.0
N2-C11.6	9.35	11.65	63.93	79.1	17.6	2.8	0.5	0.0
N2-C11.8	9.55	11.17	64.75	79.8	17.4	2.3	0.5	0.0
N2-C12.1	9.80	10.95	61.16	78.6	17.5	3.4	0.5	0.0
N2-C12.3	10.00	11.23	60.84	79.2	14.9	5.3	0.6	0.0
N2-C12.5	10.20	11.61	59.88	79.0	14.1	6.0	0.9	0.0
N2-C12.7	10.40	11.91	66.53	79.2	15.4	4.4	0.9	0.0
N2-C13.4	10.60	11.65	57.40	79.1	15.4	4.4	1.2	0.0
N2-C13.6	10.80	11.79	62.46	79.2	15.4	4.6	0.8	0.0
N2-C13.8	11.00	12.35	62.74	79.6	14.2	5.0	1.2	0.0

Table 3.4: Grain Size Measurements for N4 Samples

Sample ID Method	Depth to Sample Base (m)	Moisture Content % P1A/1	Field Moisture % N.S.	Clay % P7B/3	Silt % P7B/3	Fine Sand % P7B/3	Coarse Sand % P7B/3	Gravel % P7B/3
N4-C1.1	0.30	9.56	53.01	50.4	10.9	37.6	1.1	0.0
N4-C1.5	0.70	7.23	63.92	71.1	18.4	3.2	7.3	0.0
N4-C2.2	1.10	9.50	74.35	76.4	17.3	1.6	4.7	0.0
N4-C2.6	1.50	6.63	48.97	68.5	14.7	10.6	6.2	0.0
N4-C3.1	1.90	9.61	71.56	69.3	20.9	8.3	1.5	0.0
N4-C3.5	2.30	8.99	74.99	73.4	22.4	3.1	1.2	0.0
N4-C3.9	2.70	5.65	49.90	62.5	15.4	11.6	10.6	0.0
N4-C4.3	3.10	8.68	74.88	74.2	16.5	7.6	1.7	0.0
N4-C4.7	3.50	5.81	48.41	51.9	30.6	7.4	10.1	0.0
N4-C5.1	3.90	7.29	47.39	63.5	14.5	5.7	16.3	0.0
N4-C5.5	4.30	10.56	65.74	69.9	21.0	5.3	3.8	0.0

Table 3.4: Grain Size Measurements for N4 Samples

Sample ID Method	Depth to Sample Base (m)	Moisture Content % P1A/1	Field Moisture % N.S.	Clay % P7B/3	Silt % P7B/3	Fine Sand % P7B/3	Coarse Sand % P7B/3	Gravel % P7B/3
N4-C5.9	4.70	9.28	73.55	74.6	11.9	4.3	9.2	0.0
N4-C6.3	5.10	12.23	73.20	85.3	9.6	3.2	1.9	0.0
N4-C6.7	5.50	16.48	82.81	88.5	6.1	4.1	1.3	0.0
N4-C7.3	6.20	12.01	82.76	84.7	11.2	2.5	1.6	0.0
N4-C7.7	6.60	17.23	93.88	92.3	5.5	0.7	1.4	0.0
N4-C8.2	7.20	11.99	112.39	87.0	7.8	4.0	1.3	0.0
N4-C8.6	7.60	10.66	86.97	77.7	13.4	7.9	1.1	0.0
N4-C9.2	8.00	15.63	111.36	85.5	11.1	2.1	1.4	0.0
N4-C9.6	8.40	11.00	100.14	75.8	16.8	6.0	1.3	0.0
N4-C9.10	8.80	13.93	70.77	85.7	10.7	2.1	1.6	0.0
N4-C10.4	9.30	13.80	73.19	86.0	11.4	1.0	1.6	0.0
N4-C10.8	9.70	13.34	76.09	81.0	8.7	4.3	6.0	0.0
N4-C11.3	10.10	15.36	104.91	82.9	10.8	1.4	4.9	0.0
N4-C11.7	10.50	14.88	106.33	88.0	6.5	0.3	5.2	0.0

3.5.2 Porosity Measurements

The results of the porosity determinations for samples from bores N1, N2, and N3 are given in Table 3.5.

Table 3.5: Porosity determinations

Sample Number	Sample Depth (m)	% Moisture Content $\frac{M_l}{M_t}$	Density $\frac{M_t}{V_t}$	Porosity $\frac{V_l}{V_t}$
Bore N1				
C2.5	1.20	34.57	1540	53.48
C5.1	3.00	34.54	1590	54.92
C8.2	6.00	36.93	1380	51.00
C12.5	9.00	35.68	1490	53.17
Bore N2				
C2.1	1.15	36.49	1640	59.84
C4.7	3.20	30.03	1760	52.85
C7.1	5.30	35.80	1700	60.86
C7.7	5.90	35.20	1710	60.20
C8.4	6.50	34.12	1690	57.66
C9.3	7.35	33.98	1490	50.66
C11.9	9.65	36.61	1640	60.04
Bore N3				
C2.5	1.60	40.20	1470	59.10
C5.9	4.90	37.45	1540	57.68
C7.6	6.60	35.98	1630	60.49
C11.6	10.05	35.96	1630	58.62

3.5.3 1:5 Chemical Determinations

The results of the chemical analyses for the 1:5 extracts are presented in Table 3.6, Table 3.7, and Table 3.8 respectively. Some additional data was analysed at the WRL for the same samples on which the porosity determinations were carried out. This data is shown in Table 3.9.

Table 3.6: 1:5 Extract Chemistry for N1 Samples

Sample ID method	Sol Mg meq per 100g C10A/2	Sol Na meq per 100g C10A/2	Sol K meq per 100g C10A/2	Sol Ca meq per 100g C10A/2	CO_3 meq per 100g C12A/2	HCO_3 meq per 100g C12A/2	Cl meq per 100g C11A/1	SO_4 meq per 100g C13A/1	Avail. K meq per 100g derived
N1-C1.2	0.2	6.5	0.0	3.2	0.0	1.3	5.7	2.6	1.0
N1-C2.4	4.8	13.8	0.0	2.0	0.0	0.9	7.8	13.0	1.0
N1-C3.3	4.7	13.7	0.0	1.9	0.0	1.0	8.2	4.8	0.9
N1-C3.7	5.3	15.3	0.0	2.3	0.0	1.0	9.9	5.1	1.0
N1-C4.3	4.8	14.9	0.0	2.0	0.0	0.8	9.0	4.8	0.9
N1-C4.7	5.0	15.6	0.0	2.3	0.0	1.0	9.5	4.9	0.9
N1-C5.2	5.0	15.1	0.0	2.4	0.0	0.9	9.6	4.6	0.9
N1-C6.1	5.2	16.5	0.0	2.7	0.0	0.7	10.1	5.3	1.1
N1-C6.5	5.3	17.4	0.1	2.6	0.0	0.8	11.4	5.4	1.0
N1-C6.9	5.2	16.8	0.0	2.4	0.0	0.8	10.3	5.5	1.0
N1-C7.4	4.4	15.3	0.1	2.5	0.0	0.9	9.8	5.0	1.0
N1-C7.6	4.1	16.4	0.1	2.7	0.0	0.8	10.7	5.2	1.1
N1-C7.8	4.6	15.7	0.1	3.0	0.0	0.8	12.2	5.5	1.2
N1-C8.3	4.2	15.2	0.1	2.7	0.0	1.1	11.0	5.0	1.2
N1-C8.7	3.9	14.0	0.1	2.6	0.0	1.0	9.8	5.0	1.2
N1-C9.2	3.9	12.9	0.1	2.1	0.0	0.7	9.3	4.0	0.9
N1-C10.1	4.3	13.7	0.1	2.3	0.0	0.9	8.9	4.1	1.1
N1-C11.1	3.4	12.8	0.0	1.7	0.0	0.8	7.6	4.1	0.9
N1-C11.3	4.6	15.6	0.1	2.6	0.0	1.0	10.0	4.7	1.1
N1-C12.2	3.5	13.2	0.0	1.7	0.0	1.1	8.6	4.3	1.0
N1-C12.6	1.3	13.8	0.0	2.1	0.0	0.7	9.2	4.5	1.0

Table 3.7: 1:5 Extract Chemistry for N2 Samples

Sample ID method	Sol Mg meq per 100g C10A/2	Sol Na meq per 100g C10A/2	Sol K meq per 100g C10A/2	Sol Ca meq per 100g C10A/2	CO_3 meq per 100g C12A/2	HCO_3 meq per 100g C12A/2	Cl meq per 100g C11A/1	SO_4 meq per 100g C13A/1	Avail. K meq per 100g derived
N2-C1.2	1.1	10.1	0.0	0.5	0.0	1.6	3.8	2.8	1.3
N2-C1.4	1.1	15.3	0.0	0.3	0.0	1.6	4.6	2.8	1.2
N2-C2.2	0.8	14.0	0.0	0.2	0.0	1.7	11.2	2.8	1.3
N2-C2.4	0.6	12.3	0.0	0.2	0.0	1.6	10.1	2.8	1.2
N2-C2.6	0.8	14.7	0.0	0.3	0.0	1.8	12.3	2.8	1.1
N2-C3.2	0.7	14.1	0.0	0.3	0.0	1.6	6.4	2.8	1.1
N2-C3.4	0.7	12.3	0.0	0.2	0.0	1.5	5.5	2.8	1.0
N2-C3.6	0.7	12.2	0.0	0.2	0.0	1.5	9.5	2.8	0.9
N2-C3.8	0.6	12.2	0.0	0.2	0.0	1.5	5.0	2.8	1.0
N2-C4.2	0.5	12.2	0.0	0.2	0.0	1.6	3.5	2.8	0.9
N2-C4.4	0.6	12.4	0.0	0.2	0.7	0.0	9.5	2.8	0.9
N2-C4.6	0.5	10.6	0.0	0.2	0.0	1.3	8.3	2.7	0.6
N2-C4.8	0.5	11.0	0.0	0.2	0.0	1.4	8.4	2.7	0.6
N2-C5.2	0.9	13.1	0.0	0.3	0.0	1.4	9.8	2.7	0.7

Table 3.7: 1:5 Extract Chemistry for N2 Samples

Sample ID method	Sol Mg meq per 100g C10A/2	Sol Na meq per 100g C10A/2	Sol K meq per 100g C10A/2	Sol Ca meq per 100g C10A/2	CO_3 meq per 100g C12A/2	HCO_3 meq per 100g C12A/2	Cl meq per 100g C11A/1	SO_4 meq per 100g C13A/1	Avail. K meq per 100g derived
N2-C5.4	0.7	12.4	0.0	0.3	0.0	1.3	9.5	2.7	0.8
N2-C5.6	0.7	10.7	0.0	0.3	0.0	1.5	8.8	2.7	0.8
N2-C6.1	0.7	11.1	0.0	0.3	0.0	1.5	2.8	2.7	0.8
N2-C6.3	0.8	11.3	0.0	0.3	0.0	1.6	8.0	2.7	0.9
N2-C6.5	1.0	11.6	0.0	0.4	0.0	1.3	11.6	2.7	0.8
N2-C6.7	0.9	12.3	0.0	0.3	0.0	1.2	9.9	2.8	0.9
N2-C7.2	1.1	12.4	0.0	0.3	0.0	1.3	10.2	2.8	1.1
N2-C7.4	0.9	10.6	0.0	0.3	0.0	1.4	6.6	2.8	0.9
N2-C7.6	0.7	9.6	0.0	0.2	0.0	1.6	8.1	2.8	1.1
N2-C7.8	0.8	9.7	0.0	0.2	0.0	1.5	8.4	2.8	1.2
N2-C8.1	0.5	7.9	0.0	0.2	0.0	1.6	6.0	2.8	1.0
N2-C8.3	0.6	7.6	0.0	0.2	0.0	1.4	3.6	2.8	1.1
N2-C8.5	0.4	6.7	0.0	0.1	0.0	1.6	5.1	2.8	1.2
N2-C8.7	0.3	6.4	0.0	0.1	0.0	1.6	5.1	2.8	1.1
N2-C8.9	0.3	5.7	0.0	0.1	0.0	1.6	5.1	2.8	1.1
N2-C9.2	0.4	6.6	0.0	0.1	0.0	1.6	5.4	2.8	1.2
N2-C9.4	0.3	5.7	0.0	0.1	0.0	1.6	3.1	2.8	1.1
N2-C9.6	0.2	4.9	0.0	0.1	0.0	1.6	2.9	2.8	1.0
N2-C9.8	0.2	5.1	0.0	0.1	0.0	1.6	1.2	2.8	0.9
N2-C10.1	0.2	3.9	0.0	0.1	0.0	1.6	2.3	2.8	0.8
N2-C10.3	0.2	4.2	0.0	0.1	0.0	1.6	2.4	2.8	1.0
N2-C10.5	0.2	4.6	0.0	0.1	0.0	1.6	2.4	2.8	1.0
N2-C10.7	0.2	4.4	0.0	0.1	0.0	1.6	2.5	2.8	0.9
N2-C10.9	0.2	4.2	0.0	0.1	0.0	1.7	2.4	2.8	1.1
N2-C11.2	0.2	3.8	0.0	0.1	0.0	1.7	2.2	2.8	1.0
N2-C11.4	0.2	3.9	0.0	0.1	0.0	1.6	2.0	2.8	0.9
N2-C11.6	0.2	4.0	0.0	0.1	0.0	1.7	2.0	2.8	1.1
N2-C11.8	0.2	3.6	0.0	0.1	0.0	1.6	1.8	2.8	0.9
N2-C12.1	0.3	4.3	0.0	0.1	0.0	1.6	1.3	2.8	1.0
N2-C12.3	0.2	4.2	0.0	0.1	0.0	1.7	1.3	2.8	1.0
N2-C12.5	0.3	4.2	0.0	0.1	0.0	1.7	1.3	2.8	0.9
N2-C12.7	0.2	3.8	0.0	0.1	0.0	1.7	1.3	2.8	1.0
N2-C13.2	0.2	3.3	0.1	0.3	0.0	1.7	1.2	2.8	1.1
N2-C13.4	0.4	3.2	0.2	0.2	0.0	1.7	0.0	2.8	1.4
N2-C13.6	0.3	3.4	0.1	0.1	0.0	1.7	1.3	2.8	1.2
N2-C13.8	0.3	3.4	0.1	0.2	0.9	1.4	1.3	2.8	1.3

Table 3.8: 1:5 Extract Chemistry for N4 Samples

Sample ID method	Sol Mg meq per 100g C10A/2	Sol Na meq per 100g C10A/2	Sol K meq per 100g C10A/2	Sol Ca meq per 100g C10A/2	CO_3 meq per 100g C12A/2	HCO_3 meq per 100g C12A/2	Cl meq per 100g C11A/1	SO_4 meq per 100g C13A/1	Avail. K meq per 100g derived
N4-C1.1	2.8	2.6	0.3	4.2	1.7	2.5	5.8	0.7	1.4
N4-C1.5	0.1	0.1	0.1	0.1	1.2	1.6	2.5	0.7	0.7
N4-C2.2	0.1	0.1	0.1	0.1	1.5	6.9	0.0	0.3	1.1
N4-C2.6	0.1	4.0	0.0	0.2	0.8	3.2	0.0	0.7	0.8
N4-C3.1	0.4	2.3	0.0	0.3	0.7	3.9	0.0	0.2	1.2
N4-C3.5	0.2	1.5	0.0	0.2	0.0	2.1	0.0	0.1	1.4

Table 3.8: 1:5 Extract Chemistry for N4 Samples

Sample ID method	Sol Mg meq per 100g C10A/2	Sol Na meq per 100g C10A/2	Sol K meq per 100g C10A/2	Sol Ca meq per 100g C10A/2	CO_3 meq per 100g C12A/2	HCO_3 meq per 100g C12A/2	Cl meq per 100g C11A/1	SO_4 meq per 100g C13A/1	Avail. K meq per 100g derived
N4-C3.9	0.3	1.0	0.1	0.3	0.0	1.3	0.0	0.2	1.4
N4-C4.3	0.4	1.1	0.1	0.4	0.0	1.2	0.0	0.5	1.9
N4-C4.7	0.2	0.7	0.0	0.3	0.0	1.0	0.0	0.1	1.1
N4-C5.1	0.2	0.6	0.0	0.3	0.0	1.6	0.0	0.1	1.0
N4-C5.5	0.2	0.7	0.0	0.3	0.0	1.0	0.0	0.1	1.7
N4-C5.9	0.3	0.6	0.0	0.3	0.0	1.2	0.0	0.1	1.5
N4-C6.3	0.3	0.8	0.0	0.3	0.0	1.3	0.0	0.1	1.6
N4-C6.7	0.3	0.7	0.0	0.3	0.0	1.0	0.0	0.1	1.4
N4-C7.3	0.3	0.7	0.0	0.3	0.0	1.5	0.0	0.1	1.4
N4-C7.7	0.3	2.0	0.0	0.3	0.0	1.5	0.0	0.2	2.0
N4-C8.2	0.4	0.9	0.1	0.4	0.0	1.2	0.0	0.1	2.2
N4-C8.6	0.3	0.7	0.1	0.4	0.0	1.2	0.0	0.0	1.9
N4-C9.2	0.3	0.7	0.0	0.3	0.0	1.1	0.0	0.0	1.6
N4-C9.6	0.3	0.6	0.0	0.3	0.0	1.2	0.0	0.0	1.7
N4-C9.10	0.3	2.0	0.0	0.2	0.0	1.5	0.0	0.1	1.6
N4-C10.4	0.2	0.6	0.0	0.2	0.0	1.1	0.0	0.1	1.6
N4-C10.8	0.1	0.1	0.1	0.1	0.0	1.1	0.0	0.3	1.7
N4-C11.3	0.3	0.1	0.0	0.4	0.0	1.2	0.0	0.1	1.7

Table 3.9: 1:5 Extracts on samples used for porosity determination

Sample Number	$\sigma_{1:5}$ ($\mu S/cm$)	pH	Na^+ (mg/l)	K^+ (mg/l)	Ca^{2+} (mg/l)	Mg^{2+} (mg/l)	Cl^- (mg/l)	SO_4^{2-} (mg/l)	HCO_3^- (mg/l)	CO_3^{2-} (mg/l)
					Bore N1					
C2.5	3725	7.84	618	1.96	33.3	12.5	871	488	81	0.0
C5.1	4065	8.16	666	2.57	35.7	111	961	517	77	0.0
C8.2	4710	8.11	763	3.47	45.3	142	1182	554	80	0.0
C12.5	3840	7.94	645	2.34	29.5	94.6	912	457	79.3	0.0
					Bore N2					
C2.1	3300	8.95	673	1.34	4.73	17.0	704	361	158	8.94
C4.7	2420	8.99	495	1.26	4.10	13.0	524	226	135	9.05
C7.1	2940	8.77	583	1.74	6.98	23.6	667	280	123	4.58
C7.7	2245	8.89	449	1.41	4.33	15.5	481	209	137	5.45
C8.4	1728	8.81	343	1.24	2.61	9.07	269	113	148	6.21
C9.3	1320	9.04	267	1.23	1.96	6.79	277	66.3	154	10.13
C11.9	888	9.17	188	2.01	2.60	9.40	124	80.9	199	16.41
					Bore N3					
C2.5	525	9.32	126	0.34	1.55	3.04	20	0.0	264	25.27
C5.9	217	8.78	43	1.74	5.15	6.25	6.42	0.0	132	2.97
C7.6	486	8.64	33	3.43	6.87	11.0	4.81	0.0	116	2.01
C11.6	191	8.54	33	2.60	9.19	6.95	4.81	0.0	116.2	1.54

3.5.4 Geophysical Measurements on Core Sub-Samples

Measurements of σ_a on individual cores are shown in Table 3.10, and Table 3.11 for bores N1 and N3, and N2 respectively.

Table 3.10: $\sigma_a^{1\,kHz}$ measurements on core samples from Bores N1 & N3

Sample	Depth (m)	Bulk Conductivity mS/m
N1-C1.1	0.50	479
N1-C2.5	1.20	817
N1-C3.8	2.05	976
N1-C5.1	3.00	901
N1-C6.2	4.00	938
N1-C7.3	5.05	923
N1-C8.2	6.00	981
N1-C9.3	6.98	891
N1-C11.4	8.10	879
N1-C12.2	8.70	816
N3-C1.1	0.50	305
N3-C2.5	1.60	209
N3-C3.8	2.90	178
N3-C4.7	3.70	183
N3-C5.9	4.90	155
N3-C7.6	6.60	154
N3-C8.4	7.46	129
N3-C9.8	8.56	184

Table 3.11: Geophysical measurements on core samples from Bore N2

Sample	Depth (m)	Bulk Conductivity mS/m	Apparent Density $Kg\,m^{-3}$	P-Wave Velocity m/s
C1.1	0.45	424	1670	1514
C2.1	1.15	704	1640	1581
C2.5	1.55	725	1640	1550
C3.3	2.00	752	1660	1277
C3.7	2.40	690	1730	1546
C4.7	3.20	559	1760	1454
C5.3	3.85	671	1760	1514
C5.7	4.25	602	1780	1588
C6.4	4.75	417	1940	1843
C7.1	5.30	658	1700	1396
C7.7	5.90	581	1710	1529
C8.4	6.50	510	1690	1562
C8.8	6.90	495	1650	1532
C9.3	7.35	427	1490	1497
C9.9	7.95	378	1700	1547
C10.6	8.45	363	1670	1525
C11.3	9.05	296	1720	1601
C11.9	9.65	317	1640	1546
C12.6	10.30	302	1670	1361
C13.7	10.90	263	1670	1158

3.5.5 Hydraulic Conductivity

Crawford [5] carried out 15 falling head determinations of hydraulic conductivity on four cores. The samples were tested repeatedly after differing periods of saturation. There was a general trend for decreasing hydraulic conductivity with increasing period of saturation. The results of this testing are given in Table 3.12.

Table 3.12: Falling head hydraulic conductivity results

Sample Number	σ_w (mS/m)	Saturation (Days)	Hydraulic (m/day)
N1-8.4	1000	9	0.6
(repeat)		9	0.2
(repeat)		9	0.2
N1-8.4		10	0.5
(repeat)		10	0.08
N1-8.4	4,380	0.5	0.09
N2-4.3	1000	10	1.5
(repeat)			0.22
N2-9.1	1000	10	3.27
(repeat)			1.70
N2-9.1	1000	12	0.20
(repeat)			0.19
N3-6.9	1000	9	1.30
N3-6.9	1000	10	0.70
N3-6.9	1000	12	0.50

The fluid EC values were measured throughout each of the tests and often showed that the clay samples were not in equilibrium with the test solutions.

3.5.6 Cation Exchange Determinations

The Cation exchange data are presented in Tables 3.13, 3.14, and 3.15 respectively.

Table 3.13: EC (1:5) and Cation Exchange Capacity (CEC) Data for N1 Samples

Sample ID	EC5 dS m^{-1}	pH Water	pH $CaCl_2$	CEC meq per 100g	Ex. Mg meq per 100g	Ex. Na meq per 100g	Ex. K meq per 100g	Ex. Ca meq per 100g	E.S.P.
Method	C1A/3	C2A/2	C2A/2	C5B/2	C5B/2	C5B/2	C5B/2	C5B/2	derived
N1-C1.2	2.3	8.1	7.7	82.0	39.6	6.5	1.0	35.0	7.9
N1-C2.4	3.2	8.4	7.0	94.8	50.9	9.0	1.0	33.8	9.5
N1-C3.3	3.3	8.4	8.0	91.5	48.2	9.7	0.9	32.7	10.6
N1-C3.7	3.7	8.4	8.0	83.4	44.2	9.4	0.9	28.9	11.2
N1-C4.3	3.4	8.5	8.1	86.0	43.3	8.9	0.9	32.8	10.4
N1-C4.7	3.7	8.4	8.0	88.6	44.0	8.8	0.9	34.9	10.0
N1-C5.2	3.5	8.4	8.0	88.9	45.3	9.4	0.9	33.3	10.6
N1-C6.1	3.9	8.4	8.0	96.2	49.7	9.9	1.1	35.5	10.3
N1-C6.5	4.2	8.4	8.0	87.9	47.6	11.1	1.0	28.2	12.6
N1-C6.9	4.0	8.4	8.0	97.0	50.8	10.4	1.0	34.8	10.8

continued on next page

Table 3.13: EC (1:5) and Cation Exchange Capacity (CEC) Data for N1 Samples

Sample ID	EC5 dS m^{-1}	pH Water	pH $CaCl_2$	CEC meq per 100g	Ex. Mg meq per 100g	Ex. Na meq per 100g	Ex. K meq per 100g	Ex. Ca meq per 100g	E.S.P.
Method	C1A/3	C2A/2	C2A/2	C5B/2	C5B/2	C5B/2	C5B/2	C5B/2	derived
N1-C7.4	3.8	8.4	8.0	82.6	41.3	9.3	1.0	31.0	11.3
N1-C7.6	4.0	8.4	8.0	85.1	44.7	9.6	1.0	29.8	11.3
N1-C7.8	4.4	8.2	7.8	83.2	50.7	9.8	1.1	21.5	11.8
N1-C8.3	4.0	8.4	8.0	82.1	43.0	8.7	1.1	29.3	10.6
N1-C8.7	3.6	8.4	8.0	82.2	42.0	7.7	1.1	31.4	9.4
N1-C9.2	3.0	8.5	8.1	72.8	36.4	7.0	0.8	28.6	9.6
N1-C10.1	3.0	8.5	8.1	75.9	38.0	6.9	1.0	30.0	9.0
N1-C11.1	3.0	8.5	8.1	84.5	44.4	8.3	0.8	31.1	9.8
N1-C11.3	3.6	8.4	8.0	84.9	43.7	7.8	1.0	32.3	9.2
N1-C12.2	3.4	8.4	8.0	93.2	50.3	10.2	1.0	31.7	11.0
N1-C12.6	3.5	8.5	8.1	97.9	52.7	10.4	1.0	33.8	10.6

Table 3.14: EC (1:5) and Cation Exchange Capacity (CEC) Data for N2 Samples

Sample ID	EC5 dS m^{-1}	pH Water	pH $CaCl_2$	CEC meq per 100g	Ex. Mg meq per 100g	Ex. Na meq per 100g	Ex. K meq per 100g	Ex. Ca meq per 100g	E.S.P.
Method	C1A/3	C2A/2	C2A/2	C5B/2	C5B/2	C5B/2	C5B/2	C5B/2	derived
N2-C1.2	2.08	8.3	7.8	87.9	39.8	14.6	1.3	32.3	16.6
N2-C1.4	2.38	8.8	8.2	87.6	39.0	17.0	1.2	30.4	19.4
N2-C2.2	2.65	8.9	8.2	83.0	35.2	19.6	1.3	26.9	23.6
N2-C2.4	2.52	8.9	8.0	86.7	36.0	20.6	1.2	29.0	23.7
N2-C2.6	2.74	8.9	8.1	87.7	36.0	21.1	1.1	29.5	24.1
N2-C3.2	2.60	8.9	8.4	85.0	38.0	17.8	1.1	28.1	20.9
N2-C3.4	2.39	8.9	8.2	75.0	33.1	14.4	1.0	26.5	19.2
N2-C3.6	2.35	8.9	8.2	80.2	33.3	17.4	0.9	28.6	21.7
N2-C3.8	2.36	8.8	8.0	76.5	33.4	15.2	1.0	27.0	19.8
N2-C4.2	2.27	8.9	8.1	77.7	33.2	18.0	0.9	25.6	23.2
N2-C4.4	2.32	8.9	8.2	74.4	31.5	16.0	0.9	26.1	21.5
N2-C4.6	1.92	8.9	8.1	70.5	28.6	12.8	0.6	28.5	18.2
N2-C4.8	1.97	8.9	8.0	70.6	29.2	11.9	0.6	28.9	16.9
N2-C5.2	2.38	8.7	8.0	71.3	32.0	11.1	0.7	27.5	15.6
N2-C5.4	2.25	8.8	8.0	73.3	32.5	13.7	0.8	26.3	18.7
N2-C5.6	2.20	8.8	8.0	76.5	33.2	13.8	0.8	28.7	18.0
N2-C6.1	2.04	8.9	8.0	68.4	27.9	13.0	0.8	26.6	19.0
N2-C6.3	2.12	8.9	8.1	76.4	31.9	13.0	0.9	30.6	17.0
N2-C6.5	2.50	8.0	8.0	76.9	34.8	14.7	0.8	26.6	19.1
N2-C6.7	2.43	8.8	8.0	66.8	29.5	13.9	0.9	22.6	20.8
N2-C7.2	2.47	8.7	8.0	78.5	36.0	14.7	1.1	26.7	18.7
N2-C7.4	2.12	8.8	8.0	79.6	36.9	13.2	0.9	28.6	16.6
N2-C7.6	1.86	8.8	8.1	79.2	36.1	14.6	1.1	27.5	18.4
N2-C7.8	1.87	8.8	8.1	75.6	36.2	14.3	1.2	23.9	18.9
N2-C8.1	1.55	8.8	7.9	77.7	36.8	13.1	1.0	26.9	16.8
N2-C8.3	1.47	8.8	8.1	82.5	39.8	13.9	1.1	27.7	16.8
N2-C8.5	1.39	8.8	8.1	75.3	34.8	14.0	1.2	25.4	18.6
N2-C8.7	1.20	8.9	8.2	72.8	32.1	12.5	1.1	27.1	17.2
N2-C8.9	1.19	8.9	8.1	75.8	36.1	12.8	1.1	25.7	16.9

continued on next page

Table 3.14: EC (1:5) and Cation Exchange Capacity (CEC) Data for N2
Samples

Sample ID	EC5 dS m^{-1}	pH Water	pH $CaCl_2$	CEC meq per 100g	Ex. Mg meq per 100g	Ex. Na meq per 100g	Ex. K meq per 100g	Ex. Ca meq per 100g	E.S.P.
Method	C1A/3	C2A/2	C2A/2	C5B/2	C5B/2	C5B/2	C5B/2	C5B/2	derived
N2-C9.2	1.28	8.8	8.1	73.8	38.7	12.7	1.2	21.2	17.2
N2-C9.4	1.02	9.0	8.2	71.9	36.0	11.7	1.1	23.1	16.3
N2-C9.6	0.92	9.0	8.1	75.3	36.1	11.7	1.0	26.4	15.6
N2-C9.8	0.93	9.0	8.3	75.4	35.4	12.4	0.9	26.8	16.4
N2-C10.1	0.78	8.1	8.3	72.0	33.3	10.4	0.8	27.5	14.4
N2-C10.3	0.79	9.1	8.3	79.1	38.1	12.8	1.0	27.2	16.2
N2-C10.5	0.77	9.1	8.3	81.1	38.7	13.2	1.0	28.2	16.3
N2-C10.7	0.77	9.1	8.3	83.5	41.2	13.0	0.9	28.4	15.6
N2-C10.9	0.76	9.1	8.3	83.6	42.7	13.7	1.1	26.1	16.4
N2-C11.2	0.71	9.2	8.2	86.1	42.6	12.4	1.0	30.1	14.4
N2-C11.4	0.65	9.2	8.4	85.2	41.2	11.8	0.9	31.4	13.8
N2-C11.6	0.68	9.1	8.1	85.5	42.9	12.9	1.1	28.6	15.1
N2-C11.8	0.65	9.1	8.3	83.2	41.6	12.5	0.9	28.2	15.0
N2-C12.1	0.74	9.0	8.2	80.3	41.0	11.5	1.0	26.7	14.3
N2-C12.3	0.72	9.1	8.3	83.6	44.8	11.3	1.0	26.5	13.5
N2-C12.5	0.75	9.1	8.2	78.9	41.2	12.0	0.9	24.8	15.2
N2-C12.7	0.63	9.2	8.4	84.7	44.8	12.5	1.0	26.4	14.8
N2-C13.2	0.53	9.3	8.3	77.7	40.8	11.6	1.0	24.3	14.9
N2-C13.4	0.51	9.3	8.4	81.0	42.2	12.0	1.2	25.6	14.8
N2-C13.6	0.55	9.3	8.4	80.1	41.8	12.6	1.1	24.6	15.7
N2-C13.8	0.57	9.3	8.4	84.3	42.8	13.4	1.2	27.0	15.9

Table 3.15: EC (1:5) and Cation Exchange Capacity (CEC) Data for N4
Samples

Sample ID	EC5 dS m^{-1}	pH Water	pH $CaCl_2$	CEC meq per 100g	Ex. Mg meq per 100g	Ex. Na meq per 100g	Ex. K meq per 100g	Ex. Ca meq per 100g	E.S.P.
Method	C1A/3	C2A/2	C2A/2	C5B/2	C5B/2	C5B/2	C5B/2	C5B/2	derived
N4-C1.1	1.70	9.9	9.4	50.5	27.6	2.5	1.1	19.3	5.0
N4-C1.5	1.26	9.9	9.4	51.1	37.1	2.5	0.6	10.9	4.9
N4-C2.2	0.70	9.4	8.9	105.7	55.7	16.9	1.0	32.2	16.0
N4-C2.6	0.43	9.4	8.9	88.3	46.0	8.6	0.8	33.0	9.7
N4-C3.1	0.39	9.1	8.5	102.9	55.7	6.4	1.2	39.6	6.2
N4-C3.5	0.28	9.0	8.5	98.2	52.9	4.0	1.4	39.9	4.1
N4-C3.9	0.26	8.9	8.3	79.9	40.5	1.8	1.3	36.2	2.3
N4-C4.3	0.31	8.7	8.1	97.8	60.5	2.1	1.8	33.5	2.1
N4-C4.7	0.18	8.9	8.3	73.7	36.4	0.7	1.1	35.6	0.9
N4-C5.1	0.18	9.0	8.5	78.1	39.0	0.8	1.0	37.3	1.0
N4-C5.5	0.20	8.7	8.1	113.3	62.4	1.3	1.7	47.9	1.1
N4-C5.9	0.18	8.8	8.2	97.8	51.2	1.0	1.5	44.1	1.0
N4-C6.3	0.23	8.7	8.1	123.1	65.5	1.4	1.6	54.5	1.1
N4-C6.7	0.21	8.8	8.2	115.0	62.7	1.3	1.4	49.6	1.1
N4-C7.3	0.23	8.7	8.1	112.9	61.5	1.3	1.4	48.8	1.2
N4-C7.7	0.18	8.7	8.1	107.4	66.8	1.5	2.0	37.2	1.4
N4-C8.2	0.23	8.6	8.1	97.3	58.4	1.4	2.1	35.5	1.4
N4-C8.6	0.19	8.3	7.8	90.6	55.5	1.3	1.8	32.1	1.4
N4-C9.2	0.18	8.5	7.9	90.8	59.0	1.5	1.6	28.8	1.7

Table 3.15: EC (1:5) and Cation Exchange Capacity (CEC) Data for N4 Samples

Sample ID	EC5 dS m^{-1}	pH Water	pH $CaCl_2$	CEC meq per 100g	Ex. Mg meq per 100g	Ex. Na meq per 100g	Ex. K meq per 100g	Ex. Ca meq per 100g	E.S.P.
Method	C1A/3	C2A/2	C2A/2	C5B/2	C5B/2	C5B/2	C5B/2	C5B/2	derived
N4-C9.6	0.18	8.2	7.6	94.5	62.5	1.3	1.7	29.0	1.4
N4-C9.10	0.12	8.2	7.6	96.1	63.6	1.5	1.6	29.3	1.6
N4-C10.4	0.15	8.3	7.8	98.9	66.7	1.5	1.6	29.2	1.5
N4-C10.8	0.09	8.3	7.8	92.1	63.2	1.5	1.6	25.8	1.6
N4-C11.3	0.21	8.5	8.0	106.4	71.6	1.6	1.7	31.5	1.5
N4-C11.7	0.13	8.4	7.8	108.5	75.5	1.7	1.6	29.6	1.6

3.5.7 X-Ray diffraction Measurements

Cores from Borehole N2 were submitted for X-Ray Diffraction analysis. The results are presented in Table 3.16.

Table 3.16: X-Ray Diffraction Data for clay samples from Bore N2

Sample Depth (m)	Montmorillonite (%)	Kaolinite (%)	Quartz (%)	Plagioclase (%)	Mica (%)	Carbonate (%)
2.5	75	10	5	10	-	-
5.3	80	< 10	< 5	< 10	-	-
7.5	65	< 10	10	> 20	-	?
9.5	65	> 10	10	> 20	-	> 5
10.8	65	10	10	> 20	-	-

The major mineral phase present in all samples was a montmorillonite.

3.6 Hydrochemistry

3.6.1 Field Measurements

The field measurements made on water samples pumped from the four piezometers are presented in Table 3.17

3.6.2 Laboratory Determinations

The results of the laboratory determinations on water pumped from the four piezometers are given in Table 3.18.

Samples were also taken for stable isotope analyses from the four piezometers. This data is presented in Table 3.19. The analyses for Oxygen 18 and Deuterium were undertaken by the Adelaide Laboratory of CSIRO Land and Water.

Table 3.17: Hydrogeochemical data from Bores N1 to N4 - Field Data

Borehole Number	Temp (°C)	EC (mS/m)	pH	Eh (mV)
1	15.1	3350	7.31	104
2	16.1	1408	7.57	24
3	17.4	91.8	7.48	97
4	17.9	105.3	7.39	98

Table 3.18: Hydrogeochemical data from Bores N1 to N4 - Laboratory Data

Borehole Number	CO_2 mg/L	Na mg/L	K mg/L	Ca mg/L	Mg mg/L	Fe mg/L	HCO_3 mg/L	Cl mg/L	SO_4 mg/L
1	18.7	5,980	8.76	456	1,050	0.04	243.5	11,387	2,762
2	114.4	2,240	7.76	113.0	393	0.01	524.6	4,313	827
3	23.1	107.0	4.96	42.5	44.8	0.01	537.6	53.8	8.36
4	13.2	147.0	4.78	44.90	35.3	0.01	560.8	80.7	13.8

Table 3.19: Stable isotope analyses for water samples from Piezometers N1 to N4

Piezometer Number	δD ppm SMOW	$\delta^{18}O$ ppm SMOW
N1	-26.8	-3.08
N2	-33.3	-4.99
N3	-36.2	-5.74
N4	-36.7	-5.87

Chapter 4

INTERPRETATION

4.1 Geophysical Data

The relationship between the apparent conductivity plot (Figure 3.1) and the four EM-39 profiles with depth shows very good agreement. Bore N2 was sited on the edge of the high apparent σ_b area. The EM-39 log shows high values close to the surface, reducing with depth. The electrical conductivity image (Figure 3.10) shows a vertical slice through the area of bore N2, and confirms the distribution indicated by the EM-39 plot. The high bulk electrical conductivity material sits as a relatively thin layer on top of lower conductivity material.

The EM-31 and EM-38 surveys which were carried out at a smaller station spacing around bores N1 and N4 also show the layering in the soils. The shallow soil at bore N1 has a lower bulk electrical conductivity than the soil at similar depths around N4. This is also shown by the EM- 39 logs.

The gamma-ray activity logs show significant variation but the variation does not correlate well with any of the other physical property determinations and must be considered to be the result of small changes in the provenance of the alluvial sediments. There is no corelation between the salt content and the gamma-ray activity, indicating that the salt may have been sourced by a different sedimentological processes than those responsible for the deposition of the main body of sediment.

It is significant that there is no change in the areas of the bulk electrical conductivity anomalies between the two EM-31 survey dates. The initial survey, carried out in November, 1994 was at a coarser station spacing than the repeat survey carried out in April, 1997.

4.2 Physical Property Variation with Depth

A comprehensive data set for the study site has been assembled from the various investigations. The analysis of the individual core sub-samples has shown that the area at the top of the Yarramanbah / Pump Station Creek catchment contains uniform smectitic clay and silt to depths of greater than 10 m. There are colour variations in the cores, but no lenses of sand recorded. This is in contrast to the results reported by Acworth and Jankowski [1] for the Breeza Site.

Plots of the clay, silt, fine sand, and field moisture content are shown in Figure 4.1, Figure 4.2, Figure 4.3, and Figure 4.4 respectively. Bore N1 has a higher silt content than the other bores, and a very uniform field moisture content.
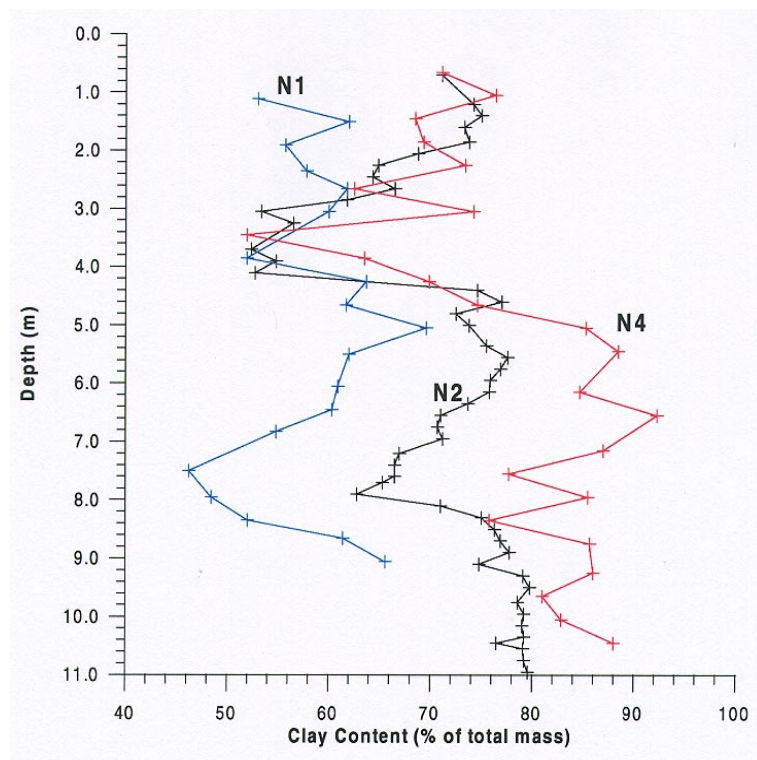
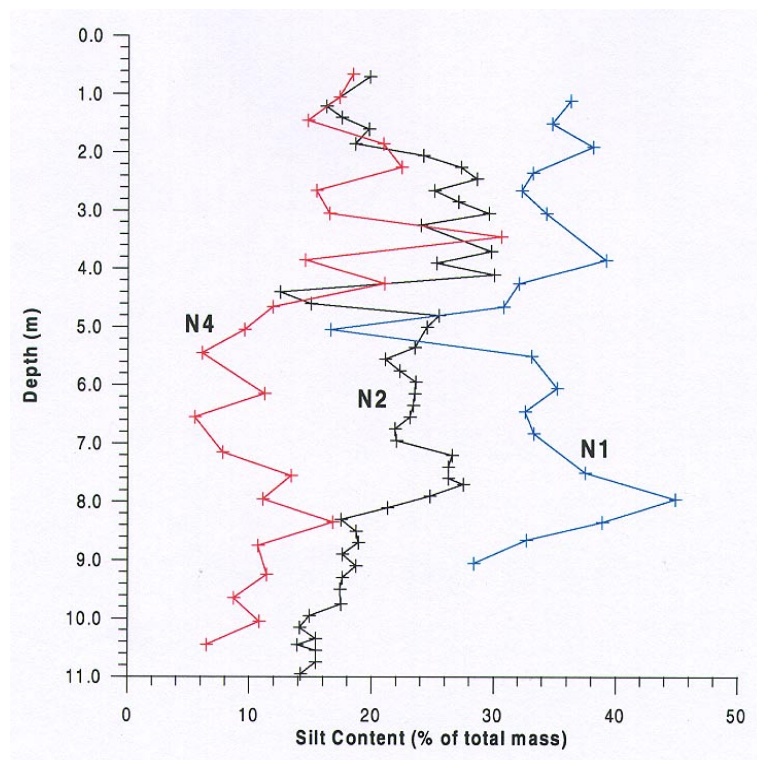Figure 4.1: Variation of clay content in bores N1, N2, and N4

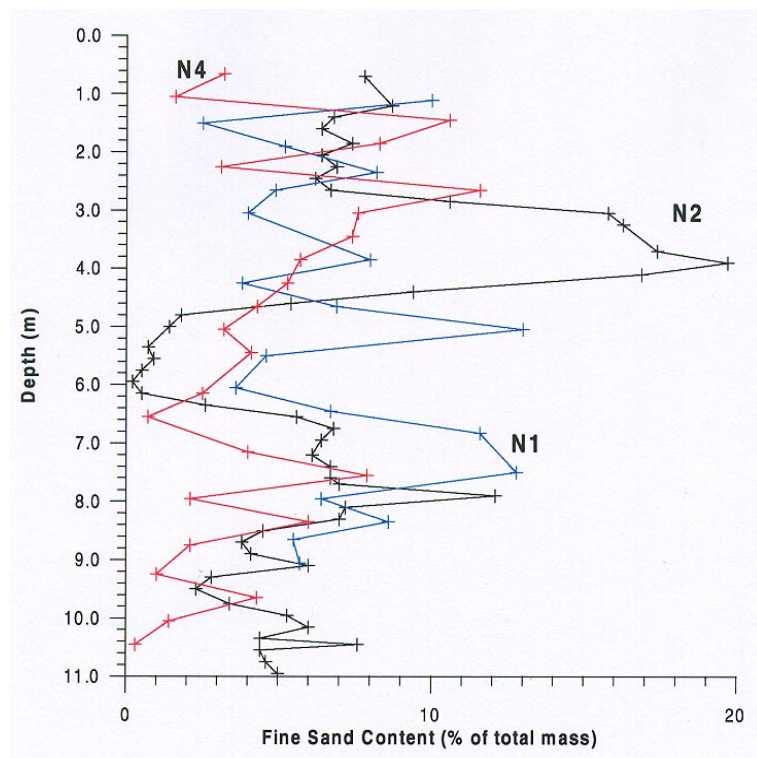Figure 4.2: Variation of silt content in bores N1, N2, and N4

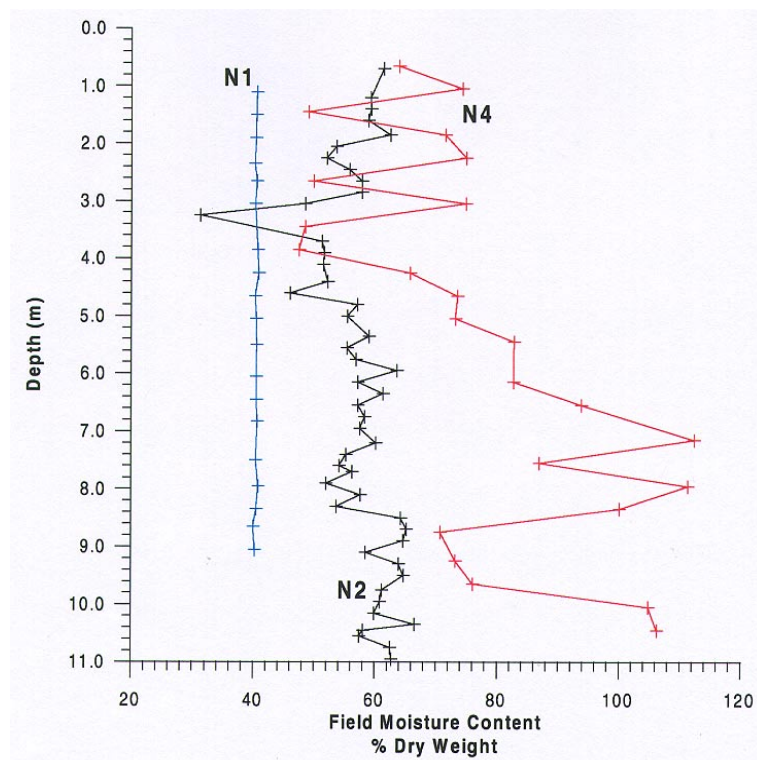Figure 4.3: Variation of fine sand content in bores N1, N2, and N4

Figure 4.4: Variation of field moisture in bores N1, N2, and N4
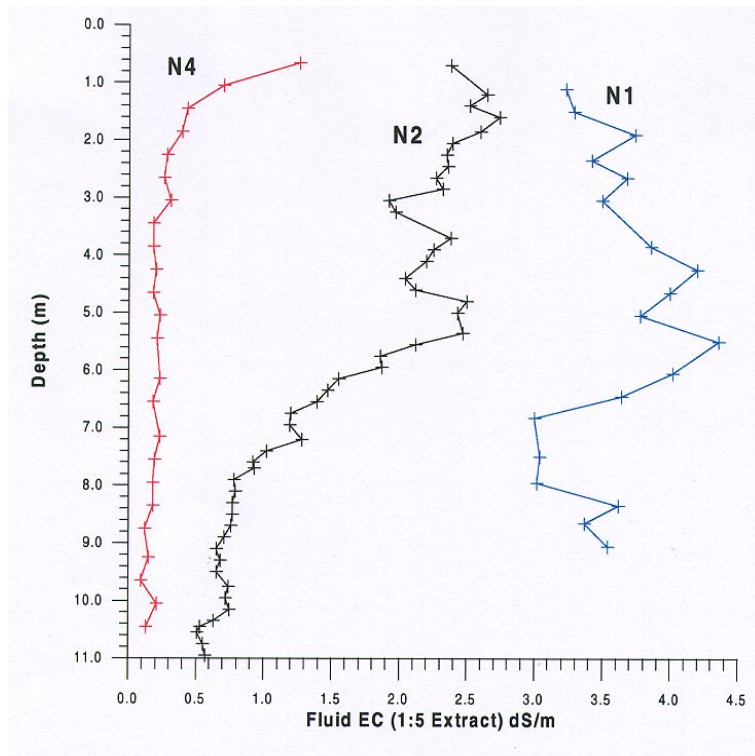
Figure 4.5: Variation of 1:5 Extract EC with Depth

The distribution of clay, silt and sand indicates a variable energy facies during sedimentation. The high percentage (20%) of fine sand mixed in with silt and clay in bore N2 at 4 m depth may indicate an aeolian component input.

The field moisture content shown in Figure 4.4 shows a remarkably uniform profile for bore N1, compared to a highly variable profile for bore N4. Moisture levels in bore N4, calculated on a per cent dry weight basis, exceed 100% for several samples at depths below 7 m.

Measurements of apparent density and seismic velocity for the bore N2 samples are also fairly uniform as shown in Table 3.11. A thin layer of higher velocity, and higher density, material at approximately 4.75m depth is not represented in the other physical property determination.

The variation of the 1:5 extract fluid σ with depth is shown in Figure 4.5. There is a clear variation between the three bores with results for N1 high; for N2 decreasing from high values at the top to lower values at the base; and values for N4 uniformly low beneath the top soil.

A plot showing the variation of total cation exchange capacity with depth for each bore is shown in Figure 4.6. Bore N4 has the greatest CEC. Individual measurements of CEC for magnesium, calcium, sodium, and potassium were carried out as listed in Tables 3.13, 3.14, and 3.15. Exchangeable potassium was low for each bore. Exchangeable sodium has low values in bore N4, similar to exchangeable potassium, but is significantly greater in bores 1 and 2. The major exchangeable ions in all the three bores analysed were magnesium and calcium, with bore N4 showing the highest levels of exchangeable ions.

4.2.1 Cross-Plot Relationships

The correlation between the individual measurements of apparent σ_b using the GEONICS EM39, and the laboratory measurements on individual core measurements (Table 3.10 and Table 3.11 refer) is shown in
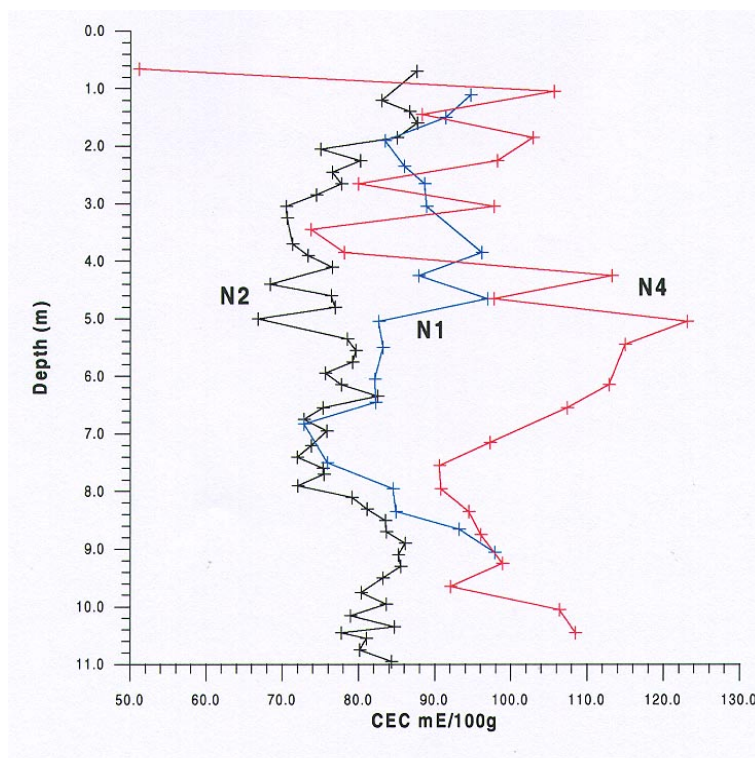
Figure 4.6: Variation of Total Cation Exchange Capacity with Depth

Figure 4.7 where results for all samples have been plotted. There is a good linear relationship (correlation coefficient of 0.934) between these variables. Scatter can be explained by taking individual measurements of σ_b from the EM-39 plots which in fact represent apparent values of σ_b due to the instrument response in the vicinity of the bore, whereas the laboratory determinations were carried out on individual cores. This data proves that the ground is fairly uniform in the vicinity of the bores.

A good exponential relationship between the σ_b values determined from the EM39 logs and the fluid EC values from analysis of the 1:5 extracts exists (Figure 4.8). The correlation coefficient for this data set is 0.956 (n=85), and is valid for a range of σ_b data between 0 and 1000 mS/m.

In contrast to the high correlation for σ_b vs σ_f for the 1:5 extracts, the correlations between σ_b and field moisture content (Figure 4.9) and σ_b and cation exchange capacity (Figure 4.10) are both very low, with no meaningful relationship evident.

Analysis of the 1:5 solution extracts shown in Table 3.6, Table 3.7, and Table 3.8 show that the major cation in the extract solutions is always sodium. A high correlation (R = 0.930) exists between the σ_b data and soluble sodium. The correlation with chloride ion is less well defined (R = 0.847) as sulphate and bicarbonate are often present in similar quantities to chloride.

4.3 Hydrochemical Data

The hydrochemical data shows that the fluids which have moved from the clays to the piezometers matches the pattern demonstrated by analysis of the 1:5 extract data. Water from piezometer 1 has a fluid electrical conductivity of 33,400 μS/cm (33.5 dS/m). Water from piezometers 3 and 4 have conductivities of 918 μS/cm (0.92 dS/m) and 1053 μS/cm (1.05 dS/m) respectively. The presence of water of such marked contrast in fluid electrical conductivity, in bores from the same depth, in a flat field with uniform
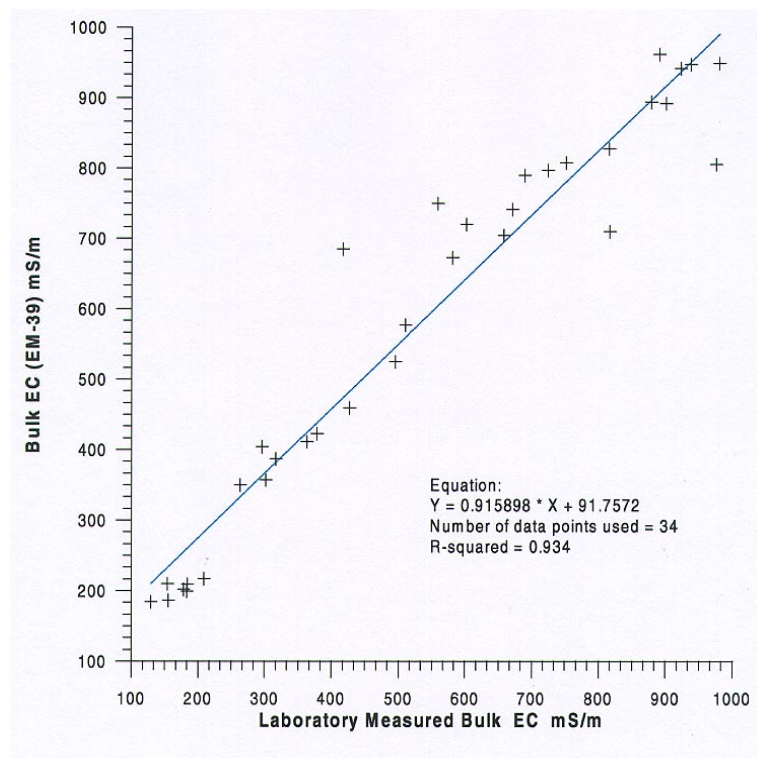
Figure 4.7: Relationship between EM-39 data and Laboratory Bulk σ_b data

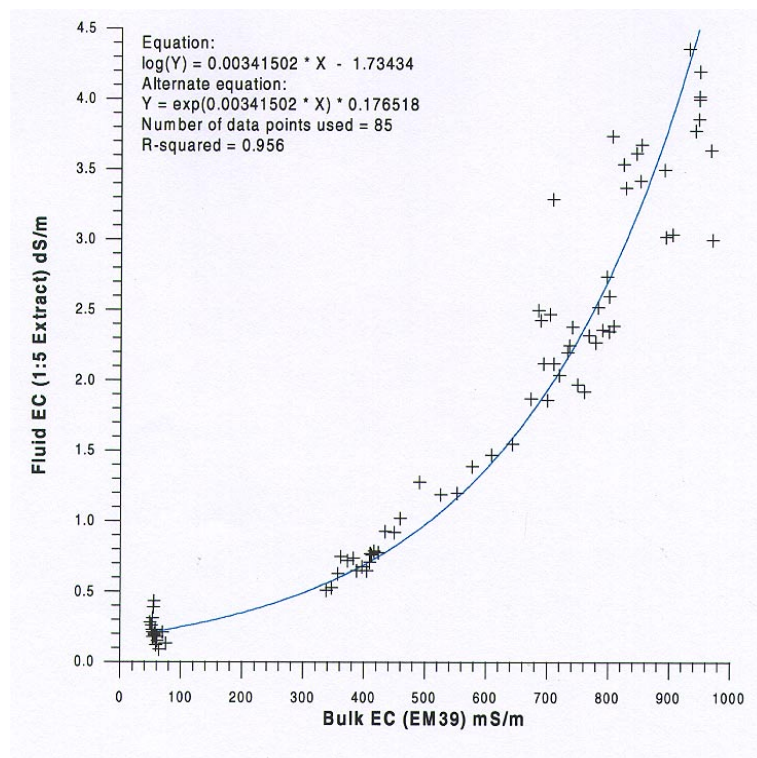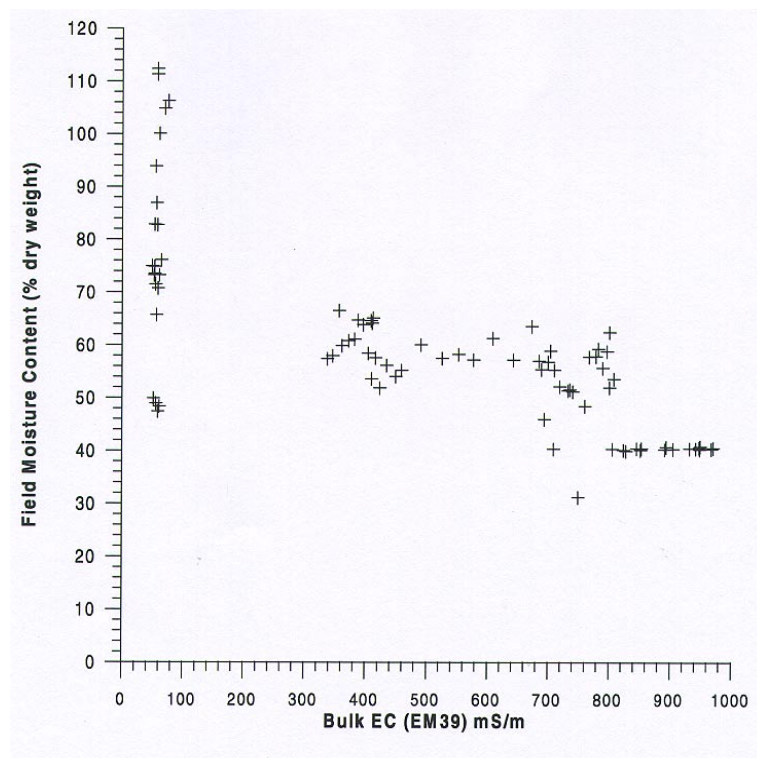Figure 4.8: Exponential relationship between σ_b (EM-39) and σ_f from 1:5 extracts

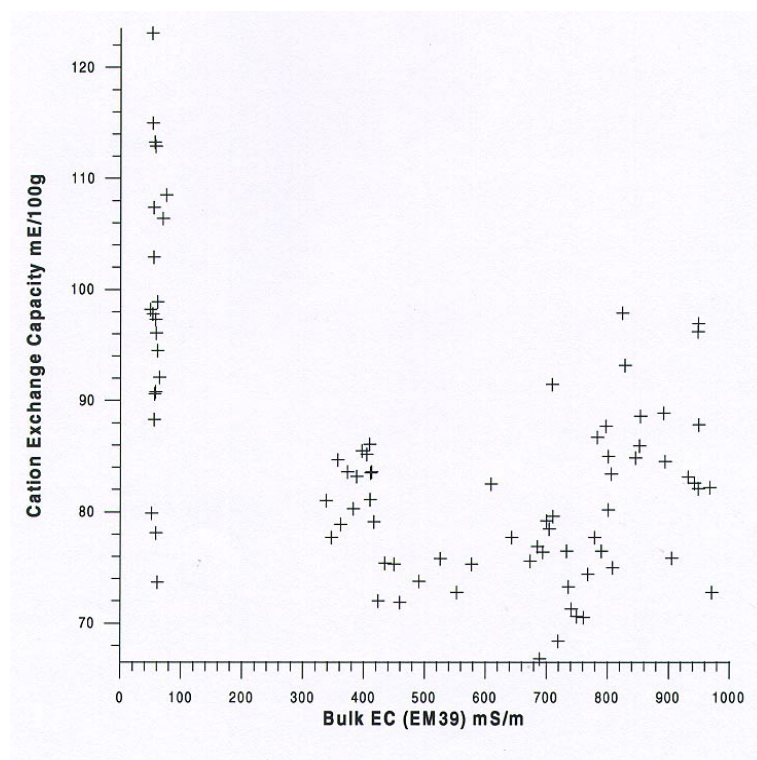Figure 4.9: Relationship between σ_b (EM-39) and Field Moisture Content

Figure 4.10: Relationship between σ_b (EM-39) and Cation Exchange Capacity

cropping, and containing a uniform smectite clay, is surprising.

Preliminary interpretation of the hydrochemical data shows that the water in bores N1 and N2 has been subject to a completely different set of chemical processes to that in bores N3 and N4. The waters represent completely different ground-water types. The Na:Cl ratio varies as 0.81, 0.80, 3.06, and 2.80 for bores N1, N2, N3, and N4 respectively. There is a major excess of Na over chloride in the cleaner bores which indicates cation exchange reactions with the clay matrix.

The oxygen deuterium data show that there is a progressive enrichment of the heavier isotopes between bores N4 and N3, through bore N2, to bore N1. This may indicate that water in bores N1 and N2 have been subject to more evaporation than bores N3 and N4 although more sampling and the establishment of a local meteoric water line for the Liverpool Plains is required before this data can be analysed more comprehensively.

Interpretation of the hydrogeochemical data indicates that water in different parts of this paddock have undergone completely different processes. This would seem to provide a strong indication that a process such as evaporative concentration can not be used to explain the occurrence of both water types, as evaporative concentration would be a uniform flux on a paddock scale. Interpretation of a more complete data set is underway.

Chapter 5

CONCLUSIONS

The cause of the sharp anomalies in bulk electrical conduction measured with the EM-31 at Yarramanbah / Pump Station Creek has been thoroughly investigated during an extensive program of surface and sub-surface geophysics, minimally disturbed core recovery and extensive physical and chemical testing of the cores.

Repeat EM-31 surveys at the test site indicate little change in the measured anomalies over the 3.5 year period between the surveys. This demonstrates that the distribution of salt in the clay has been static during this period. The sediments in the top 10 m have been sampled by continuous coring at four sites. The cores were split into 100 mm increments and grain-size determinations carried out on a large sub-set of the cores. These data show the material to be dominantly comprised of clay and silt, with moisture contents of between 40% and 110% measured on a dry weight basis. X-ray diffraction measurements show that the clay size fraction is dominantly a smectite (montmorillonite), with some secondary kaolinite. The silt fraction contained significant carbonate material in places.

Continuous profiles of bulk electrical conductivity, measured as a function of depth, were obtained using a GEONICS EM-39. These values were also confirmed by laboratory measurements of bulk electrical conductivity on individual core sub-samples.

A cross-corelation analysis between samples for bores N1, N2, and N4 indicates a high correlation between the apparent bulk electrical conductivity measured down the borehole with the EM-39 and the fluid electrical conductivity obtained from 1:5 extracts made on individual core sub-samples. Chemical analyses of the 1:5 extracts show that the changes in sodium chloride concentration in the 1:5 extracts are responsible for the majority of the change in fluid electrical conductivity.

It is interesting to note that the cation exchange capacity (CEC) is not well correlated with the bulk electrical conductivity at these sites. The CEC is uniformly high for all samples, as would be expected for samples dominated by expanding lattice clays such as the montmorillonites determined by XRD analysis. There is a similar poor correlation between bulk electrical conductivity and the field moisture content of the samples.

The silt content in Bore N1 is consistently higher, and the clay content consistently lower, than Bore N4. This may help to explain the more uniform moisture content in Bore N1, and the fact that Bore N1 has a lower moisture content than the other bores.

The changes in bulk electrical conductivity measured over the top 6 m of ground is therefore well correlated with changes in the concentration of sodium chloride in the pore space of the, otherwise uniform, clays and silts. It is important to note that this moisture is not generally free to drain from the clay, in the manner in which water would drain from a saturated sand, because it is held in the pore space by the effects of surface tension. Cores remained dry to touch even though they had moisture contents in excess

of 40%. Repeated leaching will slowly release the sodium chloride, but this will be a very slow process and will be controlled by the flux of water through the cores.

Contraction and cracking of the clays during dry periods will allow penetration of rainfall to the base of the cracked zone during storms following drought. Water pumped from the piezometers readily drains into the soil profile at all sites, indicating high values of hydraulic conductivity in the self mulching top soil. The presence of fine sand mixed with the clay in the top 4 m may possibly be explained by aeolian particles falling down cracks in the clay during dry periods.

The source of the sodium chloride, which results in such a sharp boundary between areas of high sodium chloride and areas of low sodium chloride, over an otherwise flat field with uniform lithology and land management, remains unclear. The concentration of salts from the long term discharge of ground water has been proposed as a mechanism for concentration, however, the extreme variability in salt content, both with depth, and laterally, indicates that evaporative concentration is not the main factor controlling salt distribution. Evaporation would be expected to produce a more uniform pattern of concentration in the otherwise uniform soils.

The distribution of salts within the clay indicates that the salt is an intrinsic part of the landscape. The processes which control the spatial distribution of the salt are not yet well understood. Similarly, the question of the mobility of the sodium chloride in the clays as a result of changed land management is a significant issue which requires attention.

Bibliography

[1] R.I. Acworth and J. Jankowski. The relationship between bulk electrical conductivity and dryland salinity in the Narrabri Formation at Breeza, Liverpool Plains, New South Wales, Australia. *Hydrogeology Journal*, 5(3):109–123, 1997.

[2] R.G. Banks. *Soil Landscapes of the Blackville 1:100,000 Sheet*. Department of Conservation and Land Management, New South Wales, Australia, 1996.

[3] Andrea Broughton. Mooki River Catchment Hydrogeological Investigation and Dryland Salinity Studies, The Liverpool Plains, New South Wales. Technical report, New South Wales Department of Conservation and Land Management, 1994.

[4] Andrea Broughton. The Liverpool Plains Catchment Hydrogeological Map (1:250 000 Scale). Technical report, New South Wales Department of Conservation and Land Management, 1994.

[5] R. Crawford. Hydraulic Conductivity and Mobility of Salt in Smectite Clays. Technical report, School of Civil and Environmental Engineering, The University of New South Wales, 1997. Final year - Project Report.

[6] R.H. Emmel, R.L. Stx, and J.J Sotera. Atomic Absorption Methods Manual - Standard Conditions for Flame Operation. Technical report, Instrumentation Laboratory Incorporated, 1976.

[7] G.Rayment and F.R. Higginson. *Australian Laboratory Handbook of Soil and Water Chemical Methods*. Inkata Press, 1992.

[8] D.H. Griffiths and R.D. Barker. Two-dimensional resistivity imaging and modelling in areas of complex geology. *Journal of Applied Geophysics*, 29:211–226, 1993.

[9] W.A. Jury, W.R. Gardner, and W.H. Gardner. *Soil Physics*. John Wiley & Sons, inc., fifth edition, 1991.

[10] M.H. Loke and R.D. Barker. Least squares deconvolution of apparent resistivity pseudosections. *Geophysics*, 60(6):1682–1690, 1995.

[11] M.H. Loke and R.D. Barker. Rapid least squares inversion of apparent resistivity pseudosections by a quasi-newton method. *Geophysical Prospecting*, 44:131–152, 1996.

[12] J.D. McNeil. Geonics EM39 Borehole Conductivity Meter - Theory of Operation. Technical report, Geonics Limited, 1986. TN-20.

[13] A.J. Metson. *Methods of Chemical Analysis for Soil Survey Samples*. N.Z.D.S.I.R., 1956. Soil Bureau Bulletin 12.

[14] Standards Association of Australia. Determination of the particle size distribution of a soil - an analysis by sieving in combiation with hydrometer analysis. Technical Report AS 1289 C6.2, Standards Association of Australia, 1976.

[15] Standards Association of Australia. Determination of the moisture content of a soil - oven drying method. Technical Report AS 1289 B1.1, Standards Association of Australia, 1977.

[16] N.Z. Tadros. *The Gunnedah Basin, New South Wales.* The Geological Survey of New South Wales, 1993.

[17] K.C. Taylor, J.L. Hess, and A. Mazzela. Field evaluation of a slim-line borehole induction tool. *Ground Water Monitoring Review*, 9(4):100–104, 1989.

[18] W. Timms. Liverpool Plains Water Quality Project - 1996/97 Report of Groundwater Quality. Technical report, Department of Land & Water Conservation - Centre for Natural Resources, 1997. CNR97.108.

Appendix A

Core Sub-Sample Descriptions

A.1   Borehole N1

The cores were cut into 100 mm sub-samples at the WRL. New PET caps were fixed to each sub-core. This sample set was then sub-divided for analysis.

Core from borehole N1 was split into 76 samples. The details are given in Table A.1.

Table A.1: Core Sub-Sample Descriptions for Bore N1

Sample ID	Sample Base (m)	Sample Description
N1-Cl.1	0.50	Black earth
N1-C1.2	0.60	Black earth
N1-C2.1	0.80	Red-brown clay
N1-C2.2	0.90	Red-brown clay
N1-C2.3	1.00	Red-brown clay
N1-C2.4	1.10	Red-brown clay
N1-C2.5	1.20	Dark-brown clay
N1-C3.1	1.35	Brown clay
N1-C3.2	1.45	Brown clay
N1-C3.3	1.55	Brown clay
N1-C3.4	1.65	Brown clay
N1-C3.5	1.75	Brown clay
N1-C3.6	1.85	Brown clay
N1-C3.7	1.95	Brown clay
N1-C3.8	2.05	Brown clay
N1-C4.1	2.10	Brown clay. Moist
N1-C4.2	2.20	Brown clay. Moist
N1-C4.3	2.30	Brown clay. Moist
N1-C4.4	2.40	Brown clay. Moist
N1-C4.5	2.50	Brown clay. Moist
N1-C4.6	2.60	Brown clay. Moist
N1-C4.7	2.70	Brown clay. Moist
N1-C4.8	2.80	Brown clay. Moist
N1-C4.9	2.90	Brown clay. Wet
N1-C5.1	3.00	Incomplete sample. Light brown clay
N1-C5.2	3.10	Light brown clay

Table A.1: Core Sub-Sample Descriptions for Bore N1

Sample ID	Sample Base (m)	Sample Description
N1-C5.3	3.20	Light brown clay
N1-C5.4	3.30	Light brown clay
N1-CS.5	3.40	Light brown clay
N1-C5.6	3.50	Light brown clay
N1-C5.7	3.60	Light brown clay
N1-C5.8	3.70	Light brown clay
N1-C5.9	3.80	Light brown clay
N1-C6.1	3.90	Brown clay. Moist
N1-C6.2	4.00	Brown clay. Moist
N1-C6.3	4.10	Brown clay. Moist
N1-C6.4	4.20	Brown clay. Moist
N1-C6.5	4.30	Brown clay. Moist
N1-C6.6	4.40	Brown clay. Moist
N1-C6.7	4.50	Brown clay. Moist
N1-C6.8	4.60	Brown clay. Moist
N1-C6.9	4.70	Brown clay. Moist
N1-C7.1	4.85	Incomplete sample. Brown clay
N1-C7.2	4.95	Brown clay
N1-C7.3	5.05	Brown clay
N1-C7.4	5.15	Brown clay
N1-C7.5	5.25	Brown clay
N1-C7.6	5.35	Brown clay
N1-C7.7	5.45	Brown clay
N1-C7.8	5.55	Brown clay
N1-C7.9	5.65	Brown clay
N1-C8.1	5.90	Brown clay. Moist
N1-C8.2	6.00	Brown clay. Moist
N1-C8.3	6.10	Brown clay. Moist
N1-C8.4	6.20	Brown clay. Moist
N1-C8.5	6.30	Brown clay. Moist
N1-C8.6	6.40	Brown clay. Moist
N1-C8.7	6.50	Brown clay. Moist
N1-C9.1	6.78	Brown clay. Moist
N1-C9.2	6.88	Brown clay. Moist
N1-C9.3	6.98	Brown clay. Moist
N1-C10.1	7.55	Brown clay. Wet
N1-C10.2	7.65	Brown clay. Moist
N1-C11.1	7.80	Brown clay. Moist
N1-C11.2	7.90	Brown clay. Moist
N1-C11.3	8.00	Brown clay. Moist
N1-C11.4	8.10	Brown clay. Wet
N1-C11.5	8.20	Brown clay. Wet
N1-C11.6	8.30	Brown clay. Wet
N1-C11.7	8.40	Brown clay. Moist
N1-C12.1	8.60	Dense brown clay
N1-C12.2	8.70	Dense brown clay
N1-C12.3	8.80	Dense brown clay
N1-C12.4	8.90	Dense brown clay
N1-C12.5	9.00	Dense brown clay
N1-C12.6	9.10	Dense brown clay

A.2 Borehole N2

Core from borehole N2 was split into 101 samples. The details are given in Table A.2.

Table A.2: Core Sub-Sample Descriptions for Bore N2

Sample ID	Depth to Sample Base (mm)	Sample Description
N2-C1.1	0.45	Black Earth. Cracked.
N2-C1.2	0.55	Black Earth.
N2-C1.3	0.65	Black Earth.
N2-C1.4	0.75	Black Earth. Moist.
N2-C2.1	1.15	Light brown clay. Moist.
N2-C2.2	1.25	Light brown clay. Moist.
N2-C2.3	1.35	Light brown clay. Moist.
N2-C2.4	1.45	Light brown clay. Moist.
N2-C2.5	1.55	Light brown clay. Moist.
N2-C2.6	1.65	Light brown clay. Moist.
N2-C3.1	1.80	Light brown clay. Moist.
N2-C3.2	1.90	Light brown clay. Moist.
N2-C3.3	2.00	Light brown clay. Moist.
N2-C3.4	2.10	Light brown clay. Moist.
N2-C3.5	2.20	Light brown clay. Moist.
N2-C3.6	2.30	Light brown clay. Moist.
N2-C3.7	2.40	Light brown clay. Moist.
N2-C3.8	2.50	Light brown clay. Moist.
N2-C4.1	2.60	Incomplete sample. Light brown clay. Moist.
N2-C4.2	2.70	Light brown clay. Moist.
N2-C4.3	2.80	Light brown clay. Moist.
N2-C4.4	2.90	Light brown clay. Moist.
N2-C4.5	3.00	Light brown clay. Moist.
N2-C4.6	3.10	Light brown clay. Moist.
N2-C4.7	3.20	Light brown clay. Moist.
N2-C4.8	3.30	Liqht brown clay. Moist.
N2-C5.1	3.65	Smaller diameter sample. Light brown dense clay. Moist.
N2-C5.2	3.75	Light brown dense clay. Moist.
N2-C5.3	3.85	Light brown dense clay. Moist.
N2-C5.4	3.95	Light brown dense clay. Moist.
N2-C5.5	4.05	Light brown dense clay. Moist.
N2-C5.6	4.15	Light brown dense clay. Moist.
N2-C5.7	4.25	Liqht brown dense clay. Moist.
N2-C6.1	4.45	Liqht brown dense clay. Moist.
N2-C6.2	4.55	Liqht brown dense clay. Moist.
N2-C6.3	4.65	Liqht brown dense clay. Moist.
N2-C6.4	4.75	Liqht brown dense clay. Moist.
N2-C6.5	4.85	Liqht brown dense clay. Moist.
N2-C6.6	4.95	Liqht brown dense clay. Moist.
N2-C6.7	5.05	Light brown dense clay. Moist.
N2-C6.8	5.15	Light brown dense clay. Moist.
N2-C7.1	5.30	Light brown dense clay. Moist.
N2-C7.2	5.40	Light brown dense clay. Moist.
N2-C7.3	5.50	Light brown dense clay. Moist.
N2-C7.4	5.60	Light brown dense clay. Moist.
N2-C7.5	5.70	Light brown dense clay. Moist.

Table A.2: Core Sub-Sample Descriptions for Bore N2

Sample ID	Depth to Sample Base (mm)	Sample Description
N2-C7.6	5.80	Light brown dense clay. Moist.
N2-C7.7	5.90	Light brown dense clay. Moist.
N2-C7.8	6.00	Light brown dense clay. Moist.
N2-C7.9	6.10	Light brown dense clay. Moist.
N2-C8.1	6.20	Smaller diameter sample. Light brown dense clay. Moist.
N2-C8.2	6.30	Light brown dense clay. Moist.
N2-C8.3	6.40	Light brown dense clay. Moist.
N2-C8.4	6.50	Light brown dense clay. Moist.
N2-C8.5	6.60	Light brown dense clay. Moist.
N2-C8.6	6.70	Light brown dense clay. Moist.
N2-C8.7	6.80	Liqht brown-orange dense clay. Moist.
N2-C8.8	6.90	Light brown-orange dense clay. Moist.
N2-C8.9	7.00	Liqht brown-orange dense clay. Moist.
N2-C9.1	7.15	Smaller diameter. Light brown dense clay. Moist.
N2-C9.2	7.25	Light brown dense clay. Moist.
N2-C9.3	7.35	Light brown dense clay. Moist.
N2-C9.4	7.45	Light brown dense clay. Moist.
N2-C9.5	7.55	Light brown dense clay. Moist.
N2-C9.6	7.65	Light brown dense clay. Moist.
N2-C9.7	7.75	Light brown dense clay. Moist.
N2-C9.8	7.85	Light brown dense clay. Moist.
N2-C9.9	7.95	Light brown dense clay. Moist.
N2-C10.1	7.95	Light brown dense clay. Moist.
N2-C10.2	8.05	Light brown dense clay. Moist.
N2-C10.3	8.15	Light brown dense clay. Moist.
N2-C10.4	8.25	Light brown dense clay. Moist.
N2-C10.5	8.35	Light brown dense clay. Moist.
N2-C10.6	8.45	Light brown dense clay. Moist.
N2-C10.7	8.55	Light brown dense clay. Moist. Some orange staining.
N2-C10.8	8.65	Light brown dense clay. Moist. Some orange staining.
N2-C10.9	8.75	Light brown dense clay. Moist.
N2-C11.1	8.85	Red-brown dense clay. Moist.
N2-C11.2	8.95	Red-brown dense clay. Moist.
N2-C11.3	9.05	Red-brown dense clay. Moist.
N2-C11.4	9.15	Red-brown dense clay. Moist.
N2-C11.5	9.25	Red-brown dense clay. Moist.
N2-C11.6	9.35	Red-brown dense clay. Moist.
N2-C11.7	9.45	Red-brown dense clay. Moist.
N2-C11.8	9.55	Red-brown dense clay. Moist.
N2-C11.9	9.65	Red-brown dense clay. Moist.
N2-C12.1	9.80	Light brown dense clay. Wet.
N2-C12.2	9.90	Grey-brown dense clay. Wet
N2-C12.3	10.00	Grey-brown dense clay. Wet
N2-C12.4	10.10	Grey-brown dense clay. Very wet.
N2-C12.5	10.20	Grey-brown dense clay. Wet
N2-C12.6	10.30	Grey-brown dense clay. Wet
N2-C12.7	10.40	Grey-brown dense clay. Wet
N2-C13.1	10.30	Light brown clay.
N2-C13.2	10.40	Light brown clay.
N2-C13.3	10.50	Light brown clay.
N2-C13.4	10.60	Light brown clay.

Table A.2: Core Sub-Sample Descriptions for Bore N2

Sample ID	Depth to Sample Base (mm)	Sample Description
N2-C13.5	10.70	Liqht brown clay.
N2-C13.6	10.80	Light brown clay.
N2-C13.7	10.90	Light brown clay.
N2-C13.8	11.00	Liqht brown clay.

A.3   Borehole N3

Core from borehole N3 was split into 86 samples. The details are given in Table A.3.

Table A.3: Core Sub-Sample Descriptions for Bore N3

Sample ID	Depth to Sample Base (mm)	Sample Description
N3-C1.1	0.50	Black Earth.
N3-Cl.2	0.60	Black Earth.
N3-Cl.3	0.70	Black Earth.
N3-C1.4	0.80	Light brown fine clay. Slightly moist.
N3-Cl.5	0.90	Light brown fine clay. Slightly moist.
N3-C1.6	1.00	Light brown fine clay. Slightly moist.
N3-C2.1	1.20	Light brown fine clay. Slightly moist.
N3-C2.2	1.30	Light brown fine ciay. Slightly moist.
N3-C2.3	1.40	Light brown fine ciay. Slightly moist.
N3-C2.4	1.50	Light brown fine clay. Slightly moist.
N3-C2.5	1.60	Light brown fine clay. Slightly moist.
N3-C2.6	1.70	Light brown fine clay. Slightly moist.
N3-C2.7	1.80	Light brown fine clay. Slightly moist.
N3-C2.8	1.90	Light brown fine clay. Slightly moist.
N3-C2.9	2.00	Light brown fine clay. Slightly moist.
N3-C3.1	2.20	Light brown fine clay. Slightly moist. Coarser veins throughout.
N3-C3.2	2.30	Light brown fine clay. Siightly moist. Coarser veins throughout.
N3-C3.3	2.40	Light brown fine clay. Slightly moist. Coarser veins throughout.
N3-C3.4	2.50	Light brown fine clay. Slightly moist. Coarser veins throughout.
N3-C3.5	2.60	Light brown fine clay. Slightly moist. Coarser veins throughout
N3-C3.6	2.70	Light brown fine clay. Slightly moist. Coarser veins throughout.
N3-C3.7	2.80	Light brown fine clay. Slightly moist. Coarser veins throughout.
N3-C3.8	2.90	Light brown fine clay. Siightly moist. Coarser veins throughout.
N3-C3.9	3.00	Light brown fine clay. Slightly moist. Coarser veins throughout.
N3-C4.1	3.10	9 cm sample. Light brown/grey fine clay. Mottling.
N3-C4.2	3.20	Light brown/grey fine clay. Mottling.
N3-C4.3	3.30	Light brown/grey fine clay. Mottling.
N3-C4.4	3.40	Light brown/grey fine clay. Mottling.
N3-C4.5	3.50	Light brown/grey fine clay. Mottling.
N3-C4.6	3.60	Light brown/grey fine clay. Mottling.
N3-C4.7	3.70	Light brown/grey fine clay. Mottling.
N3-C4.8	3.80	Light brown/grey fine clay. Mottling.
N3-C4.9	3.90	Light brown/grey fine clay. Mottling.

Table A.3: Core Sub-Sample Descriptions for Bore N3

Sample ID	Depth to Sample Base (mm)	Sample Description
N3-C4.10	4.00	Light brown/grey fine clay. Mottling.
N3-C5.1	4.10	11 cm sample. Light brown clay. Moist to wet.
N3-C5.2	4.20	Light brown clay. Moist to wet.
N3-C5.3	4.30	Liqht brown clay. Moist to wet.
N3-C5.4	4.40	Light brown clay. Moist to wet.
N3-C5.5	4.50	Light brown clay. Moist to wet.
N3-C5.6	4.60	Light brown clay. Moist to wet.
N3-C5.7	4.70	Light brown clay. Moist to wet.
N3-C5.8	4.80	Light brown clay. Moist to wet.
N3-C5.9	4.90	Light brown clay. Moist to wet.
N3-C5.10	5.00	Light brown clay. Moist to wet.
N3-C6.1	5.20	Light grey-brown clay. Moist but not wet. Evidence of gleying and oxidation.
N3-C6.2	5.30	Light grgy-brown cigy. Moist but not wet. Evidence of gleying snd oxidation.
N3-C6.3	5.40	Light grey-brown clay. Moist but not wet. Evidence of gleying and oxidation.
N3-C6.4	5.50	Light grey-brown clay. Moist but not wet. Evidence of gleying and oxidation.
N3-C6.5	5.60	Light grey-brown clay. Moist but not wet. Evidence of gleying and oxidation.
N3-C6.6	5.70	Light grey-brown clay. Moist but not wet. Evidence of gleying and oxidation.
N3-C6.7	5.80	Light grey-brown clay. Moist but not wet. Evidence of gleying and oxidation.
N3-C6.8	5.90	Light grey-brown clay. Moist but not wet. Evidence of gleying and oxidation.
N3-C6.9	6.00	Light grey-brown clay. Moist but not wet. Evidence of gleying and oxidation.
N3-C7.1	6.10	Light brown clay. Moist.
N3-C7.2	6.20	Light brown clay. Moist.
N3-C7.3	6.30	Light brown clay. Moist.
N3-C7.4	6.40	Light brown clay. Moist.
N3-C7.5	6.50	Light brown clay. Moist.
N3-C7.6	6.60	Light brown clay. Moist.
N3-C7.7	6.70	Light brown clay. Moist.
N3-C7.8	6.80	Light brown clay. Moist.
N3-C7.9	6.90	Light brown clay. Moist.
N3-C7.10	7.00	Light brown clay. Moist.
N3-C8.1	7.16	Light brown Clay. Moist. Coarser texture.
N3-C8.2	7.26	Light brown Clay. Moist. Coarser texture.
N3-C8.3	7.36	Light brown Clay. Moist. Coarser texture.
N3-C8.4	7.46	Light brown Clay. Moist. Coarser texture.
N3-C8.5	7.56	Light brown Clay. Moist. Coarser texture.
N3-C8.6	7.66	Light brown Clay. Moist. Coarser texture.
N3-C8.7	7.76	Light brown Clay. Moist. Coarser texture.
N3-C8.8	7.86	Light brown Clay. Moist. Coarser texture.
N3-C9.1	7.86	Light brown clay. Slightly moist.
N3-C9.2	7.96	Light brown clay. Slightly moist.
N3-C9.3	8.06	Light brown clay. Slightly moist.
N3-C9.4	8.16	Light brown clay. Slightly moist.
N3-C9.5	8.26	Light brown clay. Slightly moist.
N3-C9.6	8.36	Light brown clay. Slightly moist.
N3-C9.7	8.46	Light brown clay. Slightly moist.
N3-C9.8	8.56	Light brown clay. Slightly moist.
N3-C9.9	8.66	Light brown clay. Slightly moist.
N3-C9.10	8.76	Light brown clay. Slightly moist.
N3-C10.1	8.70	11 cm sample. Light brown clay. Moist.
N3-C10.2	8.80	Light brown clay. Moist.
N3-C10.3	8.90	Light brown clay. Moist.

Table A.3: Core Sub-Sample Descriptions for Bore N3

Sample ID	Depth to Sample Base (mm)	Sample Description
N3-C10.4	9.00	Light brown clay. Moist.
N3-C10.5	9.10	Light brown clay. Moist.

A.4 Borehole N4

Core from borehole N4 was split into 101 samples. The details are given in Table A.4.

Table A.4: Core Sub-Sample Descriptions for Bore N4

Sample ID	Depth to Sample Base (mm)	Sample Description
N4-C1.1	0.30	Friable top soil. Sample has expanded.
N4-C1.2	0.40	Friable top soil. Sample has expanded.
N4-C1.3	0.50	Friable top soil. Sample has expanded.
N4-C1.4	0.60	Light brown clay. Moist.
N4-C1.5	0.70	Light brown clay. Moist.
N4-C1.6	0.80	Light brown clay. Moist.
N4-C1.7	0.90	Light brown ciay. Moist.
N4-C2.1	1.00	Light brown clay. Moist.
N4-C2.2	1.10	Light brown clay. Moist.
N4-C2.3	1.20	Light brown clay. Moist.
N4-C2.4	1.30	Light brown clay. Moist.
N4-C2.5	1.40	Lighter creamy brown clay.
N4-C2.6	1.50	Lighter creamy brown clay.
N4-C2.7	1.60	Lighter creamy brown clay.
N4-C2.8	1.70	Lighter creamy brown clay.
N4-C2.9	1.80	Lighter creamy brown clay.
N4-C3.1	1.90	Sample only 9cm. Light creamy brown clay. Wet gravel.
N4-C3.2	2.00	Light creamy brown clay. Wet and gravel.
N4-C3.3	2.10	Light creamy brown clay. Wet and gravel.
N4-C3.4	2.20	Light creamy brown clay. Wet and gravel.
N4-C3.5	2.30	Light grey clay with darker bands. Wet.
N4-C3.6	2.40	Light grey clay with darker bands. Wet.
N4-C3.7	2.50	Light grey clay with darker bands. Wet.
N4-C3.8	2.60	Light grey clay with darker bands. Wet.
N4-C3.9	2.70	Light grey clay with darker bands. Wet.
N4-C3.10	2.80	Light grey clay with darker bands. Wet.
N4-C4.1	2.90	N4-Creamy brown clay. Mottled. Moist.
N4-C4.2	3.00	Creamy brown clay. Mottled. Moist.
N4-C4.3	3.10	Creamy brown clay. Mottled. Moist.
N4-C4.4	3.20	Creamy brown clay. Mottled. Moist.
N4-C4.5	3.30	Creamy brown clay. Mottled. Moist.
N4-C4.6	3.40	Creamy brown clay. Mottled. Moist.
N4-C4.7	3.50	Creamy brown clay. Mottled. Moist.
N4-C4.8	3.60	Creamy brown clay. Mottled. Moist.
N4-C4.9	3.70	Creamy brown clay. Mottled. Moist.

Table A.4: Core Sub-Sample Descriptions for Bore N4

Sample ID	Depth to Sample Base (mm)	Sample Description
N4-C4.10	3.80	Creamy brown clay. Mottled. Moist.
N4-C5.1	3.90	Creamy brown clay. Moist. Contains light, harder nodules.
N4-C5.2	4.00	Creamy brown clay. Moist. Contains light, harder nodules.
N4-C5.3	4.10	Creamy brown clay. Moist. Contains light, harder nodules.
N4-C5.4	4.20	Creamy brown clay. Moist. Contains light, harder nodules.
N4-C5.5	4.30	Creamy brown clay. Moist.
N4-C5.6	4.40	Creamy brown clay. Moist.
N4-C5.7	4.50	Creamy brown clay. Moist.
N4-C5.8	4.60	Creamy brown clay. Moist.
N4-C5.9	4.70	Creamy brown clay. Moist.
N4-C5.10	4.80	Creamy brown clay. Moist.
N4-C6.1	4.90	Light brown clay. Moist.
N4-C6.2	5.00	Light brown clay. Moist.
N4-C6.3	5.10	Light brown clay. Moist.
N4-C6.4	5.20	Light brown clay. Moist.
N4-C6.5	5.30	Firm clean clay.
N4-C6.6	5.40	Firm clean clay.
N4-C6.7	5.50	Firm clean clay.
N4-C6.8	5.60	Firm clean clay.
N4-C6.9	5.70	Firm clean clay.
N4-C6.10	5.80	Firm clean clay.
N4-C7.2	6.10	Light brown clay. Very wet. Some core missing.
N4-C7.3	6.20	Light brown clay. Very wet. Some core missing.
N4-C7.4	6.30	Light brown clay. Very wet. Some core missing.
N4-C7.5	6.40	Light brown clay. Moist.
N4-C7.6	6.50	Light brown clay. Moist.
N4-C7.7	6.60	Light brown clay. Moist.
N4-C7.8	6.70	Light brown clay. Moist.
N4-C7.9	6.80	Light brown clay. Moist.
N4-C8.1	7.10	Light brown clay. Very wet. Incomplete sample.
N4-C8.2	7.20	Light brown clay. Very wet. Incomplete sample.
N4-C8.3	7.30	Light brown clay. Very wet. Incomplete sample.
N4-C8.4	7.40	Light brown clay. Moist. Mottled.
N4-C8.5	7.50	Light brown clay. Moist. Mottled.
N4-C8.6	7.60	Light brown clay. Moist. Mottled.
N4-C8.7	7.70	Light brown clay. Moist. Mottled.
N4-C8.8	7.80	Light brown clay. Moist. Mottled.
N4-C8.9	7.90	cm sample. Brown clay. Coarser texture. Very moist.
N4-C9.2	8.00	Brown clay. Coarser texture. Very moist.
N4-C9.3	8.10	Brown clay. Coarser texture. Very moist.
N4-C9.4	8.20	Brown clay. Coarser texture. Moist.
N4-C9.5	8.30	Brown clay. Coarser texture. Moist.
N4-C9.6	8.40	Brown clay. Coarser texture. Moist.
N4-C9.7	8.50	Brown clay. Coarser texture. Moist.
N4-C9.8	8.60	Brown clay. Coarser texture. Moist.
N4-C9.9	8.70	Brown clay. Coarser texture. Moist.
N4-C9.10	8.80	Brown clay. Coarser texture. Moist.
N4-C10.1	9.00	Grey-brown clay. Coarser texture. Moist.
N4-C10.2	9.10	Grey-brown clay. Coarser texture. Moist.
N4-C10.3	9.20	Grey-brown clay. Coarser texture. Moist.
N4-C10.4	9.30	Grey-brown clay. Coarser texture. Moist.

Table A.4: Core Sub-Sample Descriptions for Bore N4

Sample ID	Depth to Sample Base (mm)	Sample Description
N4-C10.5	9.40	Grey-brown clay. Coarser texture. Moist.
N4-C10.6	9.50	Grey-brown clay. Coarser texture. Moist.
N4-C10.7	9.60	Grey-brown clay. Coarser texture. Moist.
N4-C10.8	9.70	Grey-brown clay. Coarser texture. Moist.
N4-C10.9	9.80	Grey-brown clay. Coarser texture. Moist.
N4-C11.1	9.90	Grey-brown clay. Coarser texture. Moist.
N4-C11.2	10.00	Grey-brown clay. Coarser texture. Moist.
N4-C11.3	10.10	Grey-brown clay. Coarser texture. Moist.
N4-C11.4	10.20	Grey-brown clay. Coarser texture. Moist.
N4-C11.5	10.30	Grey-brown clay. Coarser texture. Moist.
N4-C11.6	10.40	Grey-brown clay. Coarser texture. Moist.
N4-C11.7	10.50	Grey-brown clay. Coarser texture. Moist.
N4-C11.8	10.60	Grey-brown clay. Coarser texture. Moist.
N4-C11.9	10.70	Grey-brown clay. Coarser texture. Moist.
N4-C11.10	10.80	Grey-brown clay. Coarser texture. Moist.